STRENGTH ANALYSIS OF A SANDWICH SHELL STRUCTURE SUBJECTED TO HYDROSTATIC LOADING

by

Wonjoon Cho

Submitted to the Department of Ocean Engineering
in partial fulfillment of the requirements for the degree of

Master of Science in Naval Architecture

at the

MASSACHUSETTS INSTITUTE OF TECHNOLOGY

May 1992

Author ..... Signature redacted .....
Department of Ocean Engineering
May 8, 1992

Certified by ..... Signature redacted .....
C. Chryssostomidis
Professor of Naval Architecture
Thesis Supervisor

Accepted by ..... Signature redacted .....
A. Douglas Carmichael
Chairman, Departmental Committee on Graduate Students

STRENGTH ANALYSIS OF A SANDWICH SHELL STRUCTURE SUBJECTED TO HYDROSTATIC LOADING

by

Wonjoon Cho

Submitted to the Department of Ocean Engineering
on May 8, 1992, in partial fulfillment of the
requirements for the degree of
Master of Science in Naval Architecture

Abstract

This research investigates the static response of a circular cylindrical sandwich shell subjected to uniform external hydrostatic pressure. The sandwich shell structure is composed of two co-centric circular cylindrical shells interconnected with double V-shaped ring stiffeners.

We solve the problem by using an energy methodology which utilizes particular features of the sandwich shell structure. We formulate the complementary potential energy of the system in terms of the unknown forces and moments, developed at the structural joints of the sandwich shell. Identification of the structural equilibria is achieved by minimizing the potential energy of the system. Our methodology results in significant reduction of the dimensionality of the problem, and leads to better understanding of the relative significance of each structural component and their relative contribution to the strength of the sandwich structure.

We demonstrate that local deformations of the core stiffeners result in significant reduction of the bending phenomena close to the ends of the sandwich shell. Membrane forces developed along the meridian of the core stiffeners alter substantially the axial loading of the inner and outer shell. We compare the structural behavior of sandwich structures with first, that of monocoque cylindrical shells and second, that of ring-stiffened cylindrical shells. This comparison demonstrates the superiority of sandwich shell structures in the relief of significant loading close to rigid boundaries. Finally, the loading close to the clamped ends of the outer shell can be significantly reduced by varying the thickness distribution between the inner and outer shell.

Thesis Supervisor: C. Chryssostomidis
Title: Professor of Naval Architecture

Acknowledgments

I would like to express special thanks to my advisor Prof. C. Chryssostomidis for his guidance and support throughout the course of this work.

Also, I must mention Dr. N. Papadakis to whom I owe most of my knowledge in this research.

I am particularly grateful to my parents for their love and incessant prayers.

Contents

1 Introduction 7

2 Energy Formulation - Solution Method 10

2.1 General 10

2.2 Displacement Field of the Shells 11

2.3 Complementary Strain Energy of the Shells 14

2.4 Strain Energy of the Core Stiffeners 18

2.5 Minimization of the Total Potential Energy of the Sandwich Shell . . 21

3 Numerical Results 24

3.1 General 24

3.2 Strength Analysis of the Shells 25

3.3 Strength Analysis of the Core Stiffeners 31

3.4 Comparison between Sandwich and Ring - Stiffened Shell 33

3.5 Strength Analysis of the Sandwich Shell according to the Alteration of the Shell - Thicknesses 35

4 Conclusions and Further Studies 37

A Figures 40

B Evaluation of Energy Functions associated with Interactions between two Loads 66

Bibliography 68

List of Figures

1 A sandwich shell with double V-shaped core stiffeners 41
2 Free body diagrams of the shells 41
3 Stretching and bending energy due to a unit line force 42
4 Stretching and bending energy due to a unit line moment 42
5 Equivalent cross section and free body diagrams of the core stiffener . 43
6 Notation and sign convention 43
7 Normal displacement diagram of the sandwich shell 44
8 Longitudinal bending moment diagram of the sandwich shell 44
9 Longitudinal bending moment ($BOSOR4$) 45
10 Force resultants along the meridian of the core stiffeners 45
11 Moment resultants along the meridian of the core stiffeners 46
12 Transverse shearing force diagram of the sandwich shell 46
13 Axial load distribution along the inner and outer shell 47
14 Axial load distribution ($BOSOR4$) 47
15 Axial displacement diagram of the sandwich shell 48
16 Circumferential force resultant of the sandwich shell 48
17 Inner shell - Equivalent von Mises stress 49
18 Outer shell - Equivalent von Mises stress 49
19 Inner shell - Equivalent von Mises stress ($BOSOR4$) 50
20 Outer shell - Equivalent von Mises stress ($BOSOR4$) 50
21 Strain energy of the flanges due to local stretching 51
22 Strain energy of the flanges due to local stretching 51
23 Strain energy of the flanges due to local bending 52

24 Strain energy of the flanges due to local bending 52
25 Strain energy of the core stiffeners due to global stretching 53
26 Strain energy of the core stiffeners due to global twisting 53
27 Strain energy of the core stiffeners 54
28 Core stiffeners - Equivalent von Mises stress 54
29 Normal displacement diagram - Conventional vs sandwich shell 55
30 Bending moment diagram - Conventional vs sandwich shell 55
31 Shearing force diagram - Conventional vs sandwich shell 56
32 Circumferential force resultant - Conventional vs sandwich shell . . . 56
33 Conventional hull - Equivalent von Mises stress 57
34 Inner shell - Normal displacement diagram of the sandwich shell . . . 57
35 Outer shell - Normal displacement diagram of the sandwich shell . . . 58
36 Inner shell - Normal displacement diagram of the sandwich shell . . . 58
37 Outer shell - Normal displacement diagram of the sandwich shell . . . 59
38 Inner shell - Bending moment diagram of the sandwich shell 59
39 Outer shell - Bending moment diagram of the sandwich shell 60
40 Inner shell - Bending moment diagram of the sandwich shell 60
41 Outer shell - Bending moment diagram of the sandwich shell 61
42 Inner shell - Shearing force diagram of the sandwich shell 61
43 Outer shell - Shearing force diagram of the sandwich shell 62
44 Inner shell - Shearing force diagram of the sandwich shell 62
45 Outer shell - Shearing force diagram of the sandwich shell 63
46 Inner shell - Bending moments and shearing forces developed at the clamped ends 63
47 Outer shell - Bending moments and shearing forces developed at the clamped ends 64
48 Axial load distribution along the inner and outer shell 64
49 Axial load distribution along the inner and outer shell 65

Chapter 1

Introduction

Sandwich cylindrical shell structures are composed of two co-centric circular cylindrical shells interconnected with lightweight core. Compared with monocoque cylindrical shells, sandwich shells have the advantage that the separation of the shells increases the second moment of area of the shell structures, thus improving their ability to withstand bending in the circumferential direction and therefore buckling. The sandwich structures also provide an attractive alternative to ring-stiffened shells. The inner shell and the core stiffeners provide an elastic support for the outer shell and therefore reduce the severity of bending patterns developed in the structure.

The behavior of sandwich shell structures under hydrostatic pressure has not been investigated widely. Palaninathan and Montague [1], Montague [2], used membrane theory to estimate stresses in composite shells made of steel skins and concrete filler, subjected to hydrostatic pressure. Flugge [3] analyzed the strength of double-walled shells with circumferential and longitudinal ribs. He considered the limiting case of closely and evenly spaced ribs, stiff enough to ensure that plane sections of the double wall, orthogonal to the middle surface of the shell, remain plane after deformation. His approach leads to relatively simple numerical evaluations of the stresses and deformations of the structure, but it is not able to capture local phenomena associated with the elastic interaction between the core stiffeners and the shells.

In this thesis we describe the basic features of a structural analysis methodology, appropriate for sandwich shells subjected to axisymmetric loading. We examine the

strength of the sandwich shell structure shown in Fig. 1, with cylindrical faces and core made of the same isotropic material. Throughout this study we assume that the shell is perfect and the deformations remain in the elastic region. The lateral surface of the structure is subjected to uniform external hydrostatic pressure.

The diversity of shapes allowed by the sandwich shell geometry makes them an attractive structural device for multi-objective designs. However, it is this characteristic which makes the analysis of these structures a tedious numerical task. Due to the large number of junctions and compatibility conditions, accurate description of the deflection field requires dense discretization. Direct application of finite difference or finite element methodologies results in models with some thousand degrees of freedom. To cope with this adversity, we have developed an energy methodology which utilizes the particular geometric features of the sandwich topology shown in Fig. 1.

In Chapter 2 we describe the response of a single isotropic shell to axisymmetric line loads and moments in convenient closed-form expressions. These expressions satisfy the boundary conditions and provide an admissible deflection field. We formulate the complementary potential energy of the system in terms of the unknown forces and moments, developed at the structural joints of the sandwich shell. The strain energy of the inner and outer shell is obtained by integrating over the length of the shell. We also determine the strain energy of the core stiffeners in terms of the same unknown forces and moments. The potential energy of the entire system takes the form of a quadratic function of the unknown forces and moments. It also depends on a set of known functions representing the geometry and physical properties of the sandwich structure. Identification of the structural equilibria is achieved by minimizing the total potential energy of the system. Constraint conditions, representing local equilibria of the core stiffeners, must also be satisfied. Our methodology results in significant reduction of the dimensionality of the problem. The number of unknowns, to be determined by the minimization of the potential energy outlined before, is equal to three times the number of joints of the core stiffeners with the inner and outer shell.

In Chapter 3 we discuss numerical results obtained by the methodology outlined before. For a typical sandwich structure these results are in agreement with results

obtained using *BOSOR*4, Bushnell [4], a computer program for stress, buckling, and vibration analysis of branched shells of revolution. Furthermore, we examine the effect of the sandwich geometry on the bending patterns developed close to rigid boundaries of the sandwich shell. The analysis indicates that membrane forces developed in the flanges of the core stiffeners produce bending of the same sign to that developed at the clamped supports of the shells. This behavior of the core stiffeners results in significant reduction of the bending developed at the clamped ends along the inner and outer shell. The second distinct feature of the sandwich structure is the re-distribution of the axial loading of the inner and outer shell. Although the axial loads applied on the inner and outer shell at the boundaries are same, membrane forces applied from the core stiffeners to the shells alter significantly the axial loading of the shells. This re-distribution of the axial loads is caused by the same forces which relieve the intensity of bending close to the boundaries of the shells. We also compare the structural behavior of sandwich structures with first, that of monocoque cylindrical shells and second, that of corresponding ring-stiffened cylindrical shells. Finally, we examine the sensitivity of bending phenomena as we alter the thickness of the inner and outer shell while keeping their sum constant. The analysis indicates that the severe loading developed at the clamped boundaries of the outer shell can be significantly reduced by the alteration of the thicknesses.

In Chapter 4 we summarize the conclusions of our research and provide recommendations for the further studies.

Chapter 2

Energy Formulation - Solution Method

2.1 General

A typical sandwich cylindrical shell structure, comprising two co-centric circular cylindrical shells separated by double V-shaped core stiffeners, is shown in Fig. 1. The shape of the core stiffeners is mainly dictated by local buckling considerations, Chryssostomidis and Papadakis [13]. The central core members of the ring stiffeners provide strong supports of the V-shaped flanges, and enable the sandwich structure to withstand effectively short wavelength buckling instabilities.

In this chapter we first derive closed-form expressions for the response of a semi-infinite clamped isotropic shell, subjected to axisymmetric line loads and line moments. We next express the unknown deflection field of the sandwich shell structure in terms of the unknown forces and moments developed at the structural joints. Subsequently, the strain energy of the inner and outer shell are expressed in terms of these forces, and a set of known functions depending on the geometry of the sandwich shell. These expressions also include the effect of clamped boundaries, where bending of the shell is important. Similar expressions, describing the strain energy stored in the core members joining the inner and outer shell, are derived. Variations of the complementary potential energy can be made by changing the lateral and axial line forces,

and the line moments developed at the junctions connecting the core members and the inner and outer shell. A static conservative system is in equilibrium, if its total potential energy is stationary. Therefore, identification of the structural equilibrium corresponding to a particular value of hydrostatic pressure, can be achieved by minimizing the complementary potential energy with respect to the unknown forces and moments developed at the junctions of the sandwich shell structure.

In contrast to the existing numerical schemes, the energy approach we outline in this thesis provides an efficient way to represent the physical problem. Due to the computational efficacy of the semi-analytic approach proposed, the number of independent variables (to be determined by minimizing the potential energy) is, at most, three times the number of the structural joints. Finally, since this approach is based on closed-form expressions for the potential energy of the components of the sandwich shell, it provides further physical insight on the interaction of these members and their relative contribution to the strength of the structure.

2.2 Displacement Field of the Shells

It is known, Timoshenko and Woinowsky-Krieger [8], that the deflection $w(x)$ of an infinite isotropic cylindrical shell, due to axisymmetric line force P_j applied at longitudinal location x_j, is

$$w(x) = \frac{P_j}{8\beta^3 D}\varphi(\beta(x - x_j)), \tag{2.1}$$

$$where \quad \varphi(\beta x) = e^{-\beta|x|}(\cos(\beta x) + \sin(\beta|x|)). \tag{2.2}$$

In the above expressions D is the structural rigidity of the shell defined by

$$D = \frac{Et^3}{12(1-\nu^2)}, \tag{2.3}$$

where t, E and ν are the thickness, the Young's modulus, and the Poisson's ratio of the shell respectively. The geometric parameter β is defined by

$$\beta^4 = \frac{3(1-\nu^2)}{R^2 t^2}, \tag{2.4}$$

where R is the radius of the shell. We next derive the deflection of a semi-infinite cylindrical shell, clamped at $x = 0$, due to lateral line load P_j applied at x_j. We consider a shell of infinite extent subjected to two line loads of magnitude P_j applied at $x = \pm x_j$, and a line load of magnitude $-2P_j\varphi(\beta x_j)$, applied at $x = 0$. Employing Eq. (2. 1) we obtain :

$$w_{P_j}(x, x_j) = \frac{P_j}{8\beta^3 D}[\varphi(\beta(x - x_j)) + \varphi(\beta(x + x_j)) - 2\varphi(\beta x_j)\varphi(\beta x)] \tag{2.5}$$

It can be verified easily that expression (2. 5) satisfies the conditions of zero deflection and zero slope at $x = 0$, and it can be used to describe the response of the semi-infinite shell to the line load P_j.

The displacement of the clamped semi-infinite cylindrical shell due to an axisymmetric line moment M_j applied at x_j can be derived using Eq. (2. 5). We first consider the response of the shell to two line forces of identical magnitude and opposite signs, applied at locations x_j and x_k. This response can be evaluated using Eq. (2. 5). We then decrease distance $\Delta = x_j - x_k$ to zero and increase load P_j to infinity, while keeping $P_j\Delta = M_j$. After evaluating the appropriate limits, we derive the following expression :

$$w_{M_j}(x, x_j) = -\frac{M_j}{4\beta^2 D}[\zeta(\beta(x - x_j)) - \zeta(\beta(x + x_j)) + 2\zeta(\beta x_j)\varphi(\beta x)], \tag{2.6}$$

$$where \quad \zeta(\beta x) = e^{-\beta|x|}\sin(\beta x). \tag{2.7}$$

We note that the response of the shell to axisymmetric line load or line moment

attenuates with distance from the location of the applied load, as an exponentially damped trigonometric wave. In particular, the response of the shell is limited within distance r from the longitudinal coordinate of the applied line load or moment, given by

$$r = \frac{\pi}{\beta}. \tag{2.8}$$

The displacement of the semi-infinite clamped shell due to uniformly distributed hydrostatic pressure p is given by, Ugural [6] :

$$w_d(x) = \frac{p}{4\beta^4 D}[1 - \varphi(\beta x)]. \tag{2.9}$$

Within linear theory, the normal displacement of the outer shell w_o can be expressed as the sum of the displacement due to the external hydrostatic pressure, and the displacements due to the unknown line forces P_j's and moments M_j's, developed along the structural joints of the outer shell and the core stiffeners, i. e. :

$$w_o = w_d + \sum_{j=1}^{2N} w_{P_j} + \sum_{j=1}^{2N} w_{M_j}, \tag{2.10}$$

where N is the number of junctions between the outer shell and the core stiffeners within half length of the shell and

$$w_{P_j} = \begin{cases} w_{P_j}(x, x_j) & 1 \leq j \leq N \\ w_{P_{2N+1-j}}(L - x, L - x_j) & N+1 \leq j \leq 2N, \end{cases}$$

$$w_{M_j} = \begin{cases} w_{M_j}(x, x_j) & 1 \leq j \leq N \\ -w_{M_{2N+1-j}}(L - x, L - x_j) & N+1 \leq j \leq 2N. \end{cases}$$

We can derive the displacement field of the outer shell by substituting Eqs (2. 5), (2. 6) and (2. 9) into Eq. (2. 10). Finally, the displacement field of the inner shell can be expressed in terms of the unknown line forces and moments, developed at the

junctions between the inner shell and the core stiffeners, in a similar fashion. We note that there is no influence of the external hydrostatic pressure on the displacement field of the inner shell.

2.3 Complementary Strain Energy of the Shells

The strain energy of the outer shell U_o can be written in the form:

$$U_o = U_{bo} + U_{so}, \tag{2.11}$$

where U_{bo} is the bending energy and U_{so} is the stretching energy of the outer shell. In the case of an axisymmetrically loaded thin circular cylindrical shell, the strain energy due to bending takes the form, Ugural [6] :

$$U_{bo} = \pi R_o D_o \int_L (\frac{\partial^2 w_o}{\partial x^2})^2 dx, \tag{2.12}$$

where R_o is the radius and D_o is the structural rigidity of the outer shell. The strain energy due to axisymmetric stretching can be written in the form, Love [7] :

$$U_{so} = C_{so} \int_L (\varepsilon_{x1} + \varepsilon_{x2})^2 + 2\nu_o(\varepsilon_{x1} + \varepsilon_{x2})\varepsilon_\varphi dx, \tag{2.13}$$

where $C_{so} = \frac{\pi R_o E_o t_o}{1-\nu_o^2}$ and ν_o is the Poisson's ratio of the outer shell. Axial strains ε_{x1} and ε_{x2} are due to lateral displacement and axial loading. Strain ε_{x1} is given by

$$\varepsilon_{x1} = \nu_o \frac{w_o}{R_o}. \tag{2.14}$$

Strain ε_{x2} can be written in the form (See Fig. 2) :

$$\varepsilon_{x2} = \frac{F_{jo}}{E_o t_o}(1 - \nu_o^2). \tag{2.15}$$

F_{jo} is the axial resultant developed in the j^{th} element of the outer shell given by

$$\begin{aligned} F_{1o} &= V \\ F_{jo} &= V + \sum_{k=1}^{j-1} N_{ko} \quad for \quad j \geq 2, \end{aligned} \tag{2.16}$$

where V is the external axial loading due to hydrostatic pressure, and N_{ko} is the axial force, applied on the outer shell, at the k^{th} junction between the outer shell and the core stiffeners. The circumferential strain ε_φ is given by

$$\varepsilon_\varphi = -\frac{w_o}{R_o}. \tag{2.17}$$

Substitution of Eqs (2. 14) to (2. 17) into Eq. (2. 13) results in

$$U_{so} = 4\beta_o^4 \pi R_o D_o \int_L w_o^2 dx + \frac{2\pi R_o}{E_o t_o} \sum_{j=1}^{N+1} F_{jo}^2 l_j, \tag{2.18}$$

where l_j is the length of the j^{th} element of the shell as shown in Fig. 2. The first term in the stretching energy formulae is due to the radial deformation of the shell. The second term is the result of the axial compression or tension of the shell due to axial loads applied at the boundary and the structural joints of the shell with the core stiffeners. Expressions similar to Eqs (2. 12) and (2. 18) describe the strain energy of the inner shell U_i, in terms of its radial displacement w_i and the associated axial loading.

We next evaluate the bending and stretching energy for a finite shell of length L, in terms of the lateral line forces, line moments, and axial forces developed at the joints of the shell with the core stiffeners. Due to Saint-Venant's principle the effect of the boundary on the lateral deformation of the shell is very localized. In particular, this effect is limited within distance r from the clamped end, where r is given by Eq. (2. 8). In the following, we assume that $L > 2r$ and, therefore, there is no interaction between the left and right boundary of the finite shell. Furthermore, symmetry of the problem with respect to the middle of the shell makes it necessary to consider half length of the shell. Since deflections w_{P_j} and w_{M_j} are practically zero for $|x - x_j| > r$,

the integrals required by Eqs (2. 12) and (2. 18) can be performed over half infinite domain. Substitution of the displacement fields of the inner or outer shell into the energy formulae, results in the following integral terms :

$$(U_s)_{P_j} = 4\beta^4 \pi RD \int_0^\infty w_{P_j}^2 dx \tag{2.19}$$

$$(U_b)_{P_j} = \pi RD \int_0^\infty (\frac{\partial^2 w_{P_j}}{\partial x^2})^2 dx \tag{2.20}$$

$$(U_s)_{M_j} = 4\beta^4 \pi RD \int_0^\infty w_{M_j}^2 dx \tag{2.21}$$

$$(U_b)_{M_j} = \pi RD \int_0^\infty (\frac{\partial^2 w_{M_j}}{\partial x^2})^2 dx, \tag{2.22}$$

where w_{P_j}, w_{M_j} are given by Eqs (2. 5) and (2. 6). Functions $(U_s)_{P_j}$ and $(U_b)_{P_j}$ represent the stretching and bending energy stored in the inner or outer shell, due to axisymmetric lateral line force. Similarly, $(U_s)_{M_j}$ and $(U_b)_{M_j}$ represent the stretching and bending energy due to axisymmetric line moment. Evaluation of these integrals was performed with MACSYMA, a symbolic manipulation computer program [14]. We have

$$\begin{aligned}(U_s)_{P_j} = {} & C_P {P_j}^2 e^{-2\beta x_j}[(4\beta x_j + 3)(\cos(2\beta x_j) - 1) \\ & -3(\sin(2\beta x_j) + 1 - e^{2\beta x_j})]\end{aligned} \tag{2.23}$$

$$\begin{aligned}(U_b)_{P_j} = {} & C_P {P_j}^2 e^{-2\beta x_j}[(1 - 4\beta x_j)(\cos(2\beta x_j) - 1) \\ & -(\sin(2\beta x_j) + 1 - e^{2\beta x_j})]\end{aligned} \tag{2.24}$$

$$\begin{aligned}(U_s)_{M_j} = {} & C_M {M_j}^2 e^{-2\beta x_j}[(1 + 4\beta x_j)(\sin(2\beta x_j) - 1) \\ & +(\cos(2\beta x_j) - 1 + e^{2\beta x_j})]\end{aligned} \tag{2.25}$$

$$\begin{aligned}(U_b)_{M_j} = {} & C_M {M_j}^2 e^{-2\beta x_j}[(3 - 4\beta x_j)(\sin(2\beta x_j) - 1) \\ & +3(\cos(2\beta x_j) - 1 + e^{2\beta x_j})],\end{aligned} \tag{2.26}$$

where coefficients C_P, C_M are given by

$$C_P = \frac{\pi R}{32\beta^3 D}, \tag{2.27}$$

$$C_M = \frac{\pi R}{16\beta D}. \tag{2.28}$$

We now discuss the dependence of the energy terms, described above, on the longitudinal coordinate of the applied loads. Figs 3 and 4 show the energy per unit load stored in the shell as a function of the longitudinal coordinate of the applied load. The results have been nondimensionalized with respect to the energy stored in the shell due to a unit line force applied far away from the boundary. When a line force is applied close to the clamped boundary, the bending energy is larger than the stretching energy. However, as the applied line force moves away from the boundary, the stretching energy becomes dominant. In the case of a line moment, the bending phenomena are dominant regardless of the longitudinal coordinate of the applied line moment. As it is also shown in these figures, the magnitude of the strain energy due to line force is much larger than that of the strain energy due to line moment, provided that both loads have same numerical values. The local maxima and saddle points, characterizing the dependence of the energy on the location of the load, should be attributed to the mirror image effect of the clamped boundary. Finally, if the distance between the clamped end and the longitudinal coordinate of the applied line force or moment exceeds the value r, given by Eq. (2. 8), the energy stored in the shell is independent of the location of the line loads.

The substitution of the displacement field given by Eq. (2. 10) into the bending and stretching energy formulae results in the following :

$$(I_s)_{P_iP_j} = C_s \int_0^\infty w_{P_i} w_{P_j} dx \tag{2.29}$$

$$(I_b)_{P_iP_j} = C_b \int_0^\infty (\frac{\partial^2 w_{P_i}}{\partial x^2})(\frac{\partial^2 w_{P_j}}{\partial x^2}) dx \tag{2.30}$$

$$(I_s)_{M_iM_j} = C_s \int_0^\infty w_{M_i} w_{M_j} dx \tag{2.31}$$

$$(I_b)_{M_iM_j} = C_b \int_0^\infty (\frac{\partial^2 w_{M_i}}{\partial x^2})(\frac{\partial^2 w_{M_j}}{\partial x^2}) dx \tag{2.32}$$

$$(I_s)_{P_iM_j} = C_s \int_0^\infty w_{P_i} w_{M_j} dx \tag{2.33}$$

$$(I_b)_{P_iM_j} = C_b \int_0^\infty (\frac{\partial^2 w_{P_i}}{\partial x^2})(\frac{\partial^2 w_{M_j}}{\partial x^2}) dx \tag{2.34}$$

$$(I_s)_{pP_i} = C_s \int_0^\infty w_d w_{P_i} dx \tag{2.35}$$

$$(I_b)_{pP_i} = C_b \int_0^\infty (\frac{\partial^2 w_d}{\partial x^2})(\frac{\partial^2 w_{P_i}}{\partial x^2}) dx \tag{2.36}$$

$$(I_s)_{pM_i} = C_s \int_0^\infty w_d w_{M_i} dx \tag{2.37}$$

$$(I_b)_{pM_i} = C_b \int_0^\infty (\frac{\partial^2 w_d}{\partial x^2})(\frac{\partial^2 w_{M_i}}{\partial x^2}) dx, \tag{2.38}$$

where $C_s = 8\beta^4 \pi RD$ and $C_b = 2\pi RD$. These integrals express the strain energy stored in the shells due to the interactions among the line forces, line moments, and the distributed external hydrostatic pressure. Closed-form expressions of the strain energy associated with these interactions are presented in Appendix B. The response of axisymmetrically loaded cylindrical shells to line force or line moment is very localized. Hence, the energy due to the interaction between two line loads dies out exponentially as the distance between two loads increases. Here we introduce the parameter $r\,(= \pi/\beta)$ again and, if the distance between two line loads exceeds r, we neglect the corresponding interaction terms in the strain energy formulae. We finally note that the stretching and bending energy due to line forces, moments or their interactions are quadratic functions of the loads. However, the energy components due to the interactions between the distributed hydrostatic pressure and the line forces or moments are linear functions of the line loads.

2.4 Strain Energy of the Core Stiffeners

The deformation patterns which contribute to the strain energy of the core stiffeners are of global and local character. Since the dimensions of the ring stiffener are small compared with the radius of the sandwich structure, the double V-shaped stiffener can be considered as a thin ring undergoing global stretching and global twisting. Furthermore, a significant part of the energy stored in the stiffener, in particular when the stiffener is located close to the boundary, should be attributed to local bending and local membrane deformations of the V-shaped flanges of the stiffener.

To determine the strain energy due to global stretching, the stiffener is treated as

a thin ring subjected to line forces developed at the joints with the inner and outer shell. The equivalent cross section of the hypothetic ring has the same cross sectional area as the original ring stiffener. To simplify the notation, we denote P_1, P_2 (P_3, P_4) the unknown lateral line forces developed along the joints between the i^{th} core stiffener and the outer (inner) shell as shown in Fig. 5-(a). According to the theory of thin rings, Timoshenko and Young [9], radial force resultant T_i causes hoop tension or compression S_i, given by

$$S_i = RT_i, \tag{2.39}$$

$$where \quad T_i = P_1 + P_2 + P_3 + P_4. \tag{2.40}$$

Hence, the i^{th} core stiffener stores strain energy due to stretching, given by

$$u_{si} = \frac{\pi R}{EA} S_i^2, \tag{2.41}$$

where A is the cross sectional area of the ring stiffener.

We next determine the strain energy of the equivalent ring stiffener due to global twisting of its section. Again, to simplify the notation we denote N_1, N_2, M_1, M_2 (N_3, N_4, M_3, M_4) the axial forces and line moments developed at the joints between the core stiffener and the outer (inner) shell as shown in Fig. 5-(b). These unknown forces and moments cause an unbalanced moment with respect to the center of the stiffener. This twisting couple M_{ti} is given by

$$\begin{aligned} M_{ti} \;=\; & [P_1 - P_2 + P_3 - P_4] d \cos\alpha + \\ & [-N_1 - N_2 + N_3 + N_4](d \sin\alpha + \frac{e}{2}) + \\ & [M_1 + M_2 + M_3 + M_4]. \end{aligned} \tag{2.42}$$

Due to M_{ti}, there must be a bending moment per unit length of the ring stiffener, Timoshenko [10], given by

$$M_i = M_{ti} R. \tag{2.43}$$

Therefore, the i^{th} core stiffener stores strain energy u_{ti} given by

$$u_{ti} = \frac{\pi R}{EI_{NA}} {M_i}^2, \tag{2.44}$$

where I_{NA} is the second moment of area of the cross section with respect to the neutral axis $\overline{NA}$.

In addition to the global patterns examined before, the core stiffeners undergo local deformations. As shown in C. Chryssostomidis and N. A. Papadakis [13], if the central core member is much stiffer than the flanges of the core, the local buckling performance of the sandwich structure is significantly improved. Therefore, to compute the effect of the local phenomena on the strain energy of the core stiffeners, we consider the central core members rigid, and estimate the energy stored in the core due to the local bending and membrane deformations of the flanges. The stretching energy stored in the flanges due to the deformation along their axes can be written in the form

$$u_{ci} = \frac{\pi R d}{Es} F_{ci}^2, \tag{2.45}$$

where s and d are the thickness and length of the flange as shown in Fig. 5-(c). Force F_{ci} is given by

$$F_{ci} = P_1 \sin\alpha + N_1 \cos\alpha. \tag{2.46}$$

The unknown forces and moments, developed at the junctions between the outer shell and the core stiffeners, cause local bending of the flanges. As shown in Fig. 5-(c), the local bending moment at distance ξ from the joint of the flange with the shell is

$$m(\xi) = M_1 + [P_1 \cos\alpha - N_1 \sin\alpha]\xi. \tag{2.47}$$

Therefore, the strain energy of the core flange u_{bi} is

$$u_{bi} = \frac{\pi R}{EI} \int_0^d m^2(\xi) d\xi, \tag{2.48}$$

where I is the second moment of area with respect to the unit width of the flange

$(= \frac{s^3}{12})$.

Finally, we can determine the strain energy of the core stiffening substructure by adding the four energy components for each core stiffener and carrying out a summation over all core stiffeners.

2.5 Minimization of the Total Potential Energy of the Sandwich Shell

The complementary potential energy Π is defined by, Shames and Dym [5],

$$\Pi = U - W, \tag{2.49}$$

where U is the complementary strain energy and W is the work of the external loads. Identification of the structural equilibrium of the system can be achieved by vanishing the first variation of Π, i. e. :

$$\delta^{(1)}\Pi = \delta^{(1)}U - \delta^{(1)}W = 0. \tag{2.50}$$

Since the external loads applied on the sandwich structure are prescribed on the boundaries of the system, and no body forces are acting on the system, $\delta^{(1)}W$ vanishes identically. Accordingly, to determine unknown forces and moments at the junctions between the shells and the core stiffeners, we only need to minimize the complementary strain energy, i. e. :

$$\delta^{(1)}U = 0. \tag{2.51}$$

The complementary strain energy of the system is composed of that of the inner and outer shell and the core stiffeners. Using the methodology outlined in the previous sections, the complementary strain energy of the shells and the core stiffeners can be expressed easily in terms of the unknown forces and moments developed at the junctions between the shells and the core stiffeners. We represent the unknown forces

and moments in the vector form

$$\mathbf{f} = \{\mathbf{P_o}\ \mathbf{P_i}\ \mathbf{N_o}\ \mathbf{N_i}\ \mathbf{M_o}\ \mathbf{M_i}\}^{\mathrm{T}} \tag{2.52}$$

We denote N the number of structural joints between the outer or inner shell and the core stiffeners within half length of the sandwich shell. $\mathbf{P_o}$ ($\mathbf{P_i}$), $\mathbf{N_o}$ ($\mathbf{N_i}$), and $\mathbf{M_o}$ ($\mathbf{M_i}$) are N-dimensional row vectors representing the lateral line forces, axial line forces, and the line moments developed at the joints between the outer (inner) shell and the core stiffeners. Therefore, the complementary strain energy of the sandwich shell takes the quadratic form :

$$U = U(\mathbf{f}) = \frac{1}{2}\mathbf{f}^T\mathbf{A}\mathbf{f} + \mathbf{c}^T\mathbf{f} + const \tag{2.53}$$

The $6N$ by $6N$ matrix $\mathbf{A}$ is symmetric, positive definite and depends on the geometry of the sandwich shell. Vector $\mathbf{c}$ represents the interactions between the uniformly distributed hydrostatic pressure and the unknown line forces or moments developed in the outer shell.

The deflection fields of the shells and the core stiffeners automatically satisfy local equilibrium conditions in the radial direction. However, to obtain a well defined equilibrium, rigid body translation of the ring stiffeners along the axial direction should be prevented. Therefore, the sum of the axial forces applied on each ring stiffener has to vanish, i. e. :

$$N_1 + N_2 + N_3 + N_4 = 0. \tag{2.54}$$

Under the above observation, the minimization of the strain energy can be written in the condensed form,

$$Min.\ U(\mathbf{f})\ \ subject\ to\ \ \mathbf{C}\mathbf{f} = 0, \tag{2.55}$$

where $\mathbf{C}$ is a $\frac{N}{2}$ by $6N$ unimodular matrix, representing constraints described by Eq. (2. 54).

To complete the minimization we used the *NAG Fortran Library Routine*,

*E*04*NCF* (*NAG* [11]). *E*04*NCF* is based on the two-phase (primal) quadratic programming method, with features to exploit the convexity of the objective function. The linearity of the constraint set presents a good reason for selection of this routine. During the first phase, the method finds a feasible point by minimizing the sum of infeasibilities (feasibility phase.) Subsequently, the method minimizes the quadratic objective function within the feasible region (optimality phase.) Once any iterate is feasible, all subsequent iterates remain feasible. Since *E*04*NCF* can be used in the case that the Hessian matrix **A** is positive semi-definite, we can safely complete the minimization, despite matrix **A** being very ill-conditioned.

Chapter 3

Numerical Results

3.1 General

In this section we examine the strength of a typical sandwich shell structure with cylindrical faces and core made by the same isotropic material $Ti\text{-}4Al\text{-}4V$. The material properties are $E = 1.6\times10^7\ psi$ and $\nu = 0.32$. The hydrostatic pressure p applied on the outer shell is taken equal to 400 psi. The corresponding axial line load V, applied at the ends of the inner and outer shell, is given by

$$V = \frac{pR}{4} \approx 20000\ (lbs/in). \tag{3.1}$$

The notation and sign convention used for the force or moment resultants developed in the infinitesimal shell element is shown in Fig. 6. The dimensions of the sandwich shell are $R = 198\,in$, $L = 192\,in$, $t_i = t_o = 1\,in$, $b = 10\,in$, $e = 3.1\,in$, $q = 2s = 0.8\,in$, $d = k = 4\,in$, $l = 8\,in$, and $\alpha = 60^o$. (See Fig. 1)

Applying the energy method outlined in the last chapter, we can determine the unknown line forces, line moments, and axial forces developed at the junctions between the shells and the core stiffeners and evaluate the strength of the sandwich shell structure. Analysis of the strength of the sandwich structure was also performed using $BOSOR4$ computer program [4]. Due to the dimensionality of the problem, we were able to examine an 80 inch long shell only, in calculation by $BOSOR4$. Symmetry

of the problem with respect to the middle of the shell obviates the need to consider half length of the sandwich shell. The 80 inch shell treated by $BOSOR4$ needed close to 3000 degrees of freedom, the maximum allowed. However, for the problem under consideration, this limitation in the length is not particularly important. As we have seen in Chapter 2, the quantities that determine the bending of monocoque cylindrical shells, due to line forces and moments developed at the clamped end become small as the distance from the end of the shell exceeds the value r. In our case, the effect of the clamped supports on the bending of the inner and outer shell is limited within 35 inch from the end of the shell.

3.2 Strength Analysis of the Shells

The normal displacements of the inner and outer shell are determined by linear superposition of the deflections due to forces P_j's and moments M_j's. The deflections of the inner and outer shell are almost identical, a result of the tight cooperation of the shells enforced by the core stiffeners, as shown in Fig. 7. The slightly wavy form of the deflection curves is due to the interaction between the cylindrical shells and the core stiffeners. As the distance from the left clamped end exceeds r, the displacements of the inner and outer shells converge to 0.29 inch and they remain constant until the boundary effect of the right clamped end occurs. To justify the validity of our results, we performed evaluation of the strength of the sandwich shell using $BOSOR4$. The deflections obtained by $BOSOR4$ are shown in the same figure. Our method slightly overestimates the response of the structure. This discrepancy should be attributed to the different kinematic relations used by the two procedures. $BOSOR4$ program is based on the Novoshilov-Sanders kinematic relations appropriate for moderately large deflections.

The longitudinal bending moment M_x is given by

$$M_x = -D\frac{d^2w}{dx^2} \tag{3.2}$$

Substituting the displacement fields of the inner and outer shell into Eq. (3. 2), we obtain the bending moment distributions shown in Fig. 8. The strong wavy dependence of the bending phenomena on the longitudinal coordinate is caused by the core stiffeners. The bending moment at each clamped end of the sandwich shell reaches a value of about $-9000\ lbs \cdot in/in$. The circumferential bending moments are constant along the circumference, and their variation in the longitudinal direction can be obtained from Fig. 8, provided that the moments read from that figure are multiplied by the Poisson's ratio. The longitudinal bending moment obtained using $BOSOR4$ is shown in Fig. 9. Agreement between the results is seen to be quite good. The bending moment developed at the clamped end of a monocoque cylindrical shell, subjected to hydrostatic pressure p, is given by, Timoshenko and Woinowsky-Krieger [8] :

$$M_0 = -\frac{p}{2\beta^2}. \tag{3.3}$$

For a simple cylindrical shell with weight equal to that of the sandwich shell (i.e. of thickness $3t$), Eq. (3. 3) results in $M_0 = -74000\ lbs \cdot in/in$. This reveals a significant structural advantage of the sandwich shell structure compared with monocoque cylindrical shells. The sum of the resultant bending moments at both (inner and outer) clamped ends of the sandwich shell is about $\frac{1}{4}$ of that of the equivalent monocoque cylindrical shell.

We next discuss the effect of the geometry of the sandwich shell on the bending of the outer shell. The double V-shaped ring stiffeners close to the boundary develop strong axial loads in the direction of their flanges. The distribution of these loads along the meridian surface of the core stiffeners is given in Fig. 10. For simplicity, we restrict attention to the stiffener lying next to the clamped boundary. The leftmost flange of the stiffener lying next to the clamped boundary is stretched with tensile force of 1750 lbs/in, while its right counterpart is compressed with 4000 lbs/in. The corresponding values obtained by $BOSOR4$ are 1850 lbs/in and 3900 lbs/in, respectively. These forces, applied on the outer shell, produce a moment of the same sign to the bending moment developed at the clamped end. Line moments orthogonal

to the meridian of the core stiffeners, shown in Fig. 11, have also a similar bending effect. For instance, the V-stiffener lying next to the clamped boundary of the outer shell produces bending moments of about 1000 $lbs \cdot in/in$ and 250 $lbs \cdot in/in$ at its joints with the outer shell. The values obtained by $BOSOR4$ are 950 $lbs \cdot in/in$ and 200 $lbs \cdot in/in$, respectively. These moments are in the same direction to the moment developed at the clamped end. Therefore, the local stretching and bending of the core stiffeners close to the boundary relieve significantly the bending of the outer shell.

The transverse shearing force Q_x developed in the inner and outer shell, can be determined by

$$Q_x = -D\frac{d^3w}{dx^3}. \tag{3.4}$$

The distribution of Q_x, along the longitudinal coordinate of the inner and outer shell, is shown in Fig. 12. The discontinuities in the shear force diagram are mainly due to the membrane forces of the core stiffeners. The maximum shearing force occurs at the clamped boundary. Far away from the boundary, small shearing forces are developed in the shells. The shearing forces developed at the clamped boundary of the inner and outer shell are 2800 lbs/in and 3200 lbs/in, respectively. In the case of the equivalent monocoque cylindrical shell the shearing force developed at the clamped end is given by, Timoshenko and Woinowsky-Krieger [8] :

$$Q_0 = \frac{p}{\beta}. \tag{3.5}$$

For the equivalent monocoque cylindrical shell we obtain $Q_0 = 7700\ lbs/in$. Therefore, the sum of the resultant shearing forces at both (inner and outer) clamped ends of the sandwich shell is decreased by 22 % compared with that of the equivalent monocoque cylindrical shell.

We now examine the behavior of the structure in the longitudinal direction. The axial forces developed along the meridian of the inner and outer shell are shown in Fig. 13. Similar results obtained by $BOSOR4$ are plotted in Fig. 14. Close to the boundary, the forces applied from the core stiffeners on the shells alter significantly the axial loading of the shells. The double V-shaped stiffeners develop compression in the

outer shell and tension in the inner shell. This interaction is intense close to the ends of the shells, and dies out rapidly away from the boundary. In fact, close to the middle of the shell, the longitudinal variation of the axial load in each shell is negligible. It is important, however, that the bending close to the boundary produces a permanent effect, the re-allocation of the compressive axial load, distributed equally in the inner and outer shell at the boundary. The axial load in the outer shell is increased to the value of 25000 lbs/in ; The axial load in the inner shell is decreased to 15000 lbs/in. Therefore, the sum of the axial loads in both shells is equal to the applied axial hydrostatic load at the boundary of the structure. Direct comparison of Fig. 13 and 14 demonstrates that our results are in good agreement with those obtained with $BOSOR4$.

We next consider the axial displacements of the inner and outer shell. The axial load developed in an axisymmetrically loaded circular cylindrical shell is given by, Timoshenko and Woinowsky-Krieger [8] :

$$N_x = \frac{Et}{1-\nu^2}(\frac{du}{dx} - \nu\frac{w}{R}), \tag{3.6}$$

where u is the axial displacement of the shell. Eq. (3. 6), applied for the inner and outer shell, can be integrated along coordinate x to give the axial displacement of the shells. Since the normal displacements of the shells are almost identical, the difference between the axial deformations of the inner and outer shell, shown in Fig. 15, should be attributed to the re-allocation of the axial loading of the shells.

We now consider the forces developed in the inner and outer shells in the circumferential direction. Due to the Poisson's effect, the re-distribution of the axial loads between the inner and outer shell affects the strength of the shells in the circumferential direction as well. The circumferential force N_φ is given by, Ugural [6]:

$$N_\varphi = \frac{Et}{1-\nu^2}(-\frac{w}{R} + \nu\frac{du}{dx}). \tag{3.7}$$

Combining Eq.'s (3. 6) and (3. 7) we obtain :

$$N_\varphi = -Et(\frac{w}{R}) + \nu N_x. \tag{3.8}$$

The circumferential force resultants in the inner and outer shell are shown in Fig. 16. At the clamped end there is no normal deformation. Therefore, the circumferential force developed at the boundary is only due to the transmission of the axial load from the longitudinal to the circumferential direction, due to the Poisson's effect. As we move away from the clamped boundary, circumferential deformations, proportional to the normal deflections, increase significantly the circumferential force resultants. The difference in the circumferential forces between the inner and outer shell is due to the difference between the axial forces developed in the inner and outer shell, transmitted in the circumferential direction because of the Poisson's effect.

We next consider the equivalent von Mises stresses developed in the inner and outer shell. A realistic yield criterion considers the biaxial state of stress in the shell, Pulos and Salerno [12]. Such a criterion is the Hencky-von Mises criterion. Applying this criterion, we obtain the von Mises stress σ_Y as follows :

$$\sigma_Y = \sqrt{\sigma_x^2 + \sigma_\varphi^2 - \sigma_x \sigma_\varphi}, \tag{3.9}$$

where σ_x, σ_φ are the longitudinal and circumferential stress respectively. The longitudinal stress σ_x consists of the longitudinal membrane stress σ_{xm} and the longitudinal bending stress σ_{xb}. The circumferential stress σ_φ consists of circumferential membrane stress $\sigma_{\varphi m}$ and circumferential bending stress $\sigma_{\varphi b}$. These stresses can be estimated by the following equations, Timoshenko and Woinowsky-Krieger [8] :

$$\sigma_x = \sigma_{xm} + \sigma_{xb} \tag{3.10}$$

$$\sigma_\varphi = \sigma_{\varphi m} + \sigma_{\varphi b} \tag{3.11}$$

$$\sigma_{xm} = \frac{N_x}{t} \tag{3.12}$$

$$\sigma_{xb} = \frac{12M_x z}{t^3} \tag{3.13}$$

$$\sigma_{\varphi m} = \frac{N_\varphi}{t} \tag{3.14}$$

$$\sigma_{\varphi b} = \frac{12M_\varphi z}{t^3} \tag{3.15}$$

$$where\ z = \begin{cases} +\frac{t}{2} & \text{for the inner fiber of the shell} \\ -\frac{t}{2} & \text{for the outer fiber of the shell} \end{cases}$$

The equivalent von Mises stresses developed in the inner and outer shell are given in Fig. 17 and 18, respectively. For both shells, the maximum stress occurs in the inner fiber at the clamped boundary, where bending effects dominate membrane phenomena. Close to the boundary, bending deformations produce compressive stress in the inner fiber and tensile stress in the outer fiber. Therefore, the stresses due to the bending of the shell increase the axial compressive stress in the inner fiber, and thus the equivalent von Mises stress, and reduce the corresponding stress in the outer fiber. As we move away from the boundary, the wavy form of the longitudinal bending moments alters the sign of the bending stresses in the inner and outer fiber, and causes the wavy dependence of the von Mises stresses shown in Fig.'s 17 and 18. Far away from the boundary, the von Mises stresses are mainly due to membrane phenomena and they reach an almost constant value. The von Mises stresses in the inner and outer fiber of the outer shell is 29000 *psi*, about 3000 *psi* higher than the corresponding stresses of the inner shell. This difference is caused by the re-distribution of the axial loading in the inner and outer shell discussed earlier in this section. The equivalent von Mises stresses obtained by $BOSOR4$ are given in Fig.'s 19 and 20. Agreement between the results obtained by two methodologies is quite good.

3.3 Strength Analysis of the Core Stiffeners

The light weight core interconnecting the inner and outer shell is an essential part of the sandwich shell structure and withstands a significant part of the applied hydrostatic pressure. The forces developed along the meridian of the core stiffeners are shown in Fig. 10. Their role on the relief of the severe bending close to the boundary, as well as, their substantial influence on the axial loading of the inner and outer shell, has been discussed in the previous section. The comparison of the sandwich structure with the equivalent monocoque cylindrical shell has also demonstrated the important role of the core stiffeners.

We now examine the global stretching of the core stiffeners mentioned in Section 2. 4. The sum of the lateral line forces, applied on the core stiffener through the structural joints, causes the global stretching, hoop tension or compression given by Eq. (2. 39). In the case of the stiffener lying next to the clamped boundary, the equivalent line force applied on the core stiffener is 113 lbs/in radially inwards. Therefore, applying this to Eq. (2. 39) we obtain 22000 lbs of hoop compression. As we move away from the boundary, the equivalent line forces applied on the core stiffeners have always radially inward directions and the magnitudes of the forces are increased to the value of about 1000 lbs/in. Therefore, far away from the boundary, large and almost constant value of hoop compressions, the value of about 200000 lbs, occur in the core stiffeners.

Line forces, moments and axial forces applied on the core stiffener from the inner and outer shell cause the unbalanced moment M_{ti}, distributed uniformly along the circumference of the ring stiffener, as illustrated in Section 2. 4. The unbalanced moment is given by Eq. (2. 42). For the ring stiffener next to the clamped end, the unbalanced moment has the value of 27 $lbs \cdot in/in$. Accordingly, the bending moment per unit length of the ring stiffener is 124 $lbs \cdot in$ by Eq. (2. 43). The torsional rigidity of the ring stiffeners contributes to the bending rigidity of the sandwich shell structure and to the reduction of the bending moments developed at the clamped ends. However, as we move away from the boundary, it converges to zero.

The bending moments developed along the meridian of the core stiffeners are shown in Fig. 11. The stiffeners located close to the clamped boundaries develop significant moments along the junctions with the inner and outer shell and hence, they play an important role on the relief of the bending moments developed at the clamped ends. We can also predict the bending moment developed along the circumference of the core stiffeners which is the result of the transmission of the meridional bending caused by the Poisson's ratio.

Owing to the characteristic of our energy formulation, we can analyze each energy component which constitutes the strain energy of the core stiffeners. We first examine the strain energy of the core stiffeners due to local compression (or tension). From Fig. 21 and 22, we can see that relatively large amount of local compression (or tension) is developed in the core stiffeners close to the boundaries. Most of the energy due to local compression (or tension) is stored in the left members of the core stiffeners connected with the outer shell and in the right members of the stiffeners connected with the inner shell. As we move away from the boundary, the difference of the energy stored in the left and right members decreases and the strain energy of the core stiffeners due to local compression (or tension) also decreases and finally becomes negligible. The core stiffener lying next to the clamped boundary stores 14000 $lbs \cdot in$ of strain energy due to this phenomenon, which is 17 % of the total strain energy stored in that stiffener. However, far away from the boundary, only 1600 $lbs \cdot in$ of the energy is developed due to local compression. As shown in Fig. 27, the total strain energy stored in the core stiffener located far away from the boundary is approximately 230000 $lbs \cdot in$. Therefore, the contribution of the local compression to the strain energy of the core stiffener is negligible far away from the clamped ends.

Fig. 23 and 24 illustrate the effect of the local bending of the core members on the strain energy of the stiffeners. In the case of the core stiffener lying next to the clamped end, 66000 $lbs \cdot in$ of the strain energy is developed due to local bending of the core members, which is 80 % of the total strain energy stored in that stiffener (See also Fig. 27). This result demonstrates the significant role of the local bending phenomena, due to the particular geometry of the double V-shaped ring stiffeners,

on the structural behaviors of the sandwich shell closed to the clamped boundaries. Same figures also show that the local bending effect dies out rapidly far away from the boundaries.

Strain energy stored in each core stiffeners due to global stretching is shown in Fig. 25. The core stiffener lying next to the clamped end stores 2200 $lbs \cdot in$ of the strain energy due to this phenomena, which is only 3 % of the total energy stored in that stiffener. However, as we move away from the boundary, global stretching becomes dominant and almost all of the strain energy of the core stiffeners is due to this global stretching as shown in Fig. 25 and 27.

As it is shown in Fig. 26, global twisting is limited close to the boundaries. However, only negligible portion of the strain energy is caused by the global twisting compared with the total strain energy stored in the core stiffeners.

The stresses developed along the inner fiber of the stiffeners are shown in Fig. 28. Close to the boundary, local stretching and local bending phenomena result in the maximum stress of about 65000 psi. Far away from the boundary, the stresses due to global stretching phenomena dominate, and the stresses decrease to about 20000 psi.

3.4 Comparison between Sandwich and Ring - Stiffened Shell

We now compare the typical sandwich shell structure, examined earlier in this chapter, with an equivalent ring-stiffened cylindrical shell. We consider a single isotropic shell with radius equal to the radius of the outer shell. The shell is reinforced with equidistant ring stiffeners, spaced 36 inch apart. The shell and the stiffeners are made of steel with Young's modulus 3.0×10^7 psi and Poisson's ratio 0.29. The thickness of the shell is 1.15 inch. The thickness and the length of the flange (web) are 2.1 (0.88) inch and 9.3 (13.2) inch, respectively. We notice that both structures have the same weight per unit length. To analyze the conventional hull structure, we used the methodology presented in Chapter 2. In the case of the ring-stiffened shell, there is no variation in the axial loading along the meridian of the shell. Furthermore, it is only

global stretching and global twisting of the stiffeners which contribute to the strength of the stiffeners. The flexural rigidity EI_{NA}, which restrains the global twisting of the ring stiffeners is, $4.4 \times 10^9\ lbs \cdot in^2$, about thirty times larger than that of the double V-shaped ring stiffeners.

The normal displacement of the conventional hull and the sandwich shell structure are shown in Fig. 29. Due to the concentrated line forces and moments applied from the sparsely distributed ring stiffeners to the shell, the normal displacement of the conventional hull structure has a pronounced wavy form. The longitudinal bending moment and the transverse shearing force distributions are shown in Fig. 30, 31 respectively. Due to the sparsely distributed ring stiffeners, the bending moment distribution has periodic form with period equal to the spacing of the stiffeners. Sharp troughs occur at the structural joints, and smooth crests appear near the middle of adjacent junctions. The maximum bending moment, developed at the clamped boundary, is $-27000\ lbs{\cdot}in/in$, 1.5 times larger than the sum of the maximum bending moments developed in the inner and outer shell of the sandwich shell structure.

We next consider the circumferential force resultant of the conventional hull structure. The circumferential force resultant is given by Eq. (3. 8). In the case of conventional hull structure, the axial force resultant N_x is constant (40000 psi) along the longitudinal coordinate and, therefore, the variation in the circumferential force resultant is only due to the normal displacement of the shell. As it is shown in Fig. 32, the wavy variation of the circumferential force resultant along the longitudinal coordinate is similar to that of the normal displacement distribution, shown in Fig. 29.

The equivalent von Mises stresses developed in the inner and outer fiber of the conventional hull structure are shown in Fig. 33. Similar to the case of sandwich shell structure, the maximum stress occurs in the inner fiber at the clamped boundary, where bending dominates membrane phenomena. The maximum equivalent von Mises stress is 140000 psi, about 2 times greater than the corresponding stress developed in the sandwich shell. This result is primarily due to the severe bending developed at the clamped end of the traditional ring-stiffened structure.

3.5 Strength Analysis of the Sandwich Shell according to the Alteration of the Shell - Thicknesses

In this section we consider the influence of the thickness alteration of the inner and outer shell on the sandwich shell structures. For this investigation, we keep the sum of the thickness of the inner and outer shell constant, 2 in, i. e. :

$$t_i + t_o = 2. \tag{3.16}$$

First, we consider the case in which t_i's are 1, 1.2 and 1.4 in and the corresponding t_o's are 1, 0.8 and 0.6 in. We next decrease the thickness of the inner shell to 1, 0.8 and 0.6 in and increase the thickness of the outer shell to 1, 1.2 and 1.4 in respectively.

The normal displacements of the inner and outer shell for each case are shown in Figs 34 to 37. From these figures, we can see that, as the thickness of the outer shell increases, the displacements of the inner and outer shell decrease slightly. This result should be attributed to the different geometry of the shells and the way they sustain the normal deflection caused by hydrostatic pressure. Furthermore, the displacement of the thin shell is wavier. This is caused by the fact that as the thickness of the shell is decreased, its flexibility is increased and therefore, the thin shell easily responds to the line loads applied from the core stiffeners through the structural joints.

The longitudinal bending moments and transverse shearing forces developed in the inner and outer shell are shown in Figs 38 to 45. It is worth paying attention to the bending moments and shearing forces developed at the clamped boundaries of the shells. In all cases, larger value of bending moment and shearing force are developed in the thicker shell (whether it is inner or outer). This phenomenon is more clearly explained in Figs 46 and 47. We can also see that, as the thickness of the inner shell is increased, the sum of the shearing forces of the inner and outer shell which is applied to the end boundaries (bulkheads) is decreased. This analysis indicates that we can relieve even further the bending moment and shearing force at the clamped end of

the outer shell and the sum of the transverse shearing resultants at the bulkhead by properly increasing the thickness of the inner shell in comparison with that of the outer shell.

We now examine the axial load distributions along the meridian of the shells for each case. As shown in Figs 48 and 49, the re-distribution of the axial loading is significantly influenced by the alteration of the thicknesses of the inner and outer shell. In the case $t_i > t_o$, as the thickness of the inner shell is increased, the difference in the axial loading between the inner and outer shell close to the clamped ends is decreased. Furthermore, as we move away from the boundary, the difference in the axial loading is increased and reaches its maximum value near the $x = \pi/\beta_o$. However, as we move even further away from the boundary that difference begins to decrease and converges to some value. As it is also shown in Fig. 48, in the case that the thickness of the outer shell is much smaller than that of the inner shell, larger axial loading is developed in the inner shell far away from the boundary. The longitudinal dependence of the axial loading, in the case $t_i < t_o$, is shown in Fig. 49. As the thickness of the inner shell is increased, the difference in the axial loading between the inner and outer shell is increased and the behavior of the axial loading along the meridian of the shells is similar to that of the representative case $t_i = t_o = 1\ in.$

Chapter 4

Conclusions and Further Studies

We have investigated strength of submerged sandwich shell structures which are composed of two co-centric circular cylindrical shells and double V-shaped ring stiffeners. Our research is primarily focused on the structural phenomena close to the rigid supports (king frames or bulkheads). In the following we summarize the important results of this research and provide some recommendations for the further studies.

Our analysis is based on the energy methodology which utilizes the particular geometric features of sandwich shells. The potential energy of the system is decomposed to the energy of the inner and outer shell and the energy components of the core. To obtain the response of the system to axisymmetric external loading, the energy function is minimized with respect to the unknown forces and moments developed at the structural joints between the shells and core stiffeners. The first advantage of this approach is that it provides a very efficient algorithmic process and reduces enormously the dimensionality of the problem. Even more importantly, it provides an indispensible tool for structural analysis and leads to better understanding of the relative significance of each structural component and its contribution to the behavior of sandwich shell structures.

Owing to the characteristic of our energy formulation, we can analyze the relative significance of each energy components stored in the double V-shaped ring stiffeners. Close to the rigid boundaries, local bending and local compression (or tension) phenomena of the ring stiffeners are dominant. These two phenomena play an impor-

tant role on the relief of the significant bending developed at the clamped boundaries. However, as we move away from the boundaries, almost all of the strain energy stored in the core stiffeners is due to the global stretching phenomena. The reduction of the bending moments and shearing forces developed at the rigid supports is a particularly attractive feature of the sandwich structure. This behavior would certainly have serious dynamic implications. Since the intensity of the transmitted forces and moments to the rigid ends is small, so must be the intensity of the motion of these ends excited by dynamic deformation patterns propagating in the shells. Further analytic and numerical efforts along this direction are necessary.

Due to the coupling between the axial and lateral deformations, the double V-shaped ring stiffeners produce axial compressions in the outer shell and tensions in the inner shell through their structural joints. This out of phase axial loading of the shells is one of the major characteristics of sandwich shell structures. Dynamic implications of this behavior need to be further analyzed. Although the nonlinear nature of this interaction is a source of additional analytic and computational complexity, our basic energy formulation could be extended to examine the possibility of further reduction of the lateral displacements and accelerations of the outer shell.

We have compared the longitudinal bending moment and the transverse shearing force developed in the representative sandwich shell with those developed in the conventional hull structure (a single shell with equidistant ring stiffeners). Since both shell structures have the same weight per unit length and are subjected to the same hydrostatic loading, they seem to have similar strength characteristics. However, much smaller bending moments are developed in the sandwich shell structure.

The distribution of the bending moment and the transverse shearing force along the inner and outer shell can be modified by altering the thickness of each shell. We have examined the bending moments and the shearing forces developed in the shells with the thickness of the outer (inner) shell reduced (increased) from 1.4 (0.6) to 0.6 (1.4) inches. According to the results, the bending moment and the shearing force developed at the clamped end of the outer shell are significantly reduced as the thickness of the outer shell is decreased. This analysis demonstrates that the weight

allocation between the inner and outer shell provides an additional degree of freedom to reduce the intensity of bending patterns propagating in the outer shell and the transmission of energy to the surrounding environment. Finally, the out of phase axial loading phenomena in the inner and outer shell can be significantly influenced by the alteration of the shell-thicknesses.

Appendix A

Figures

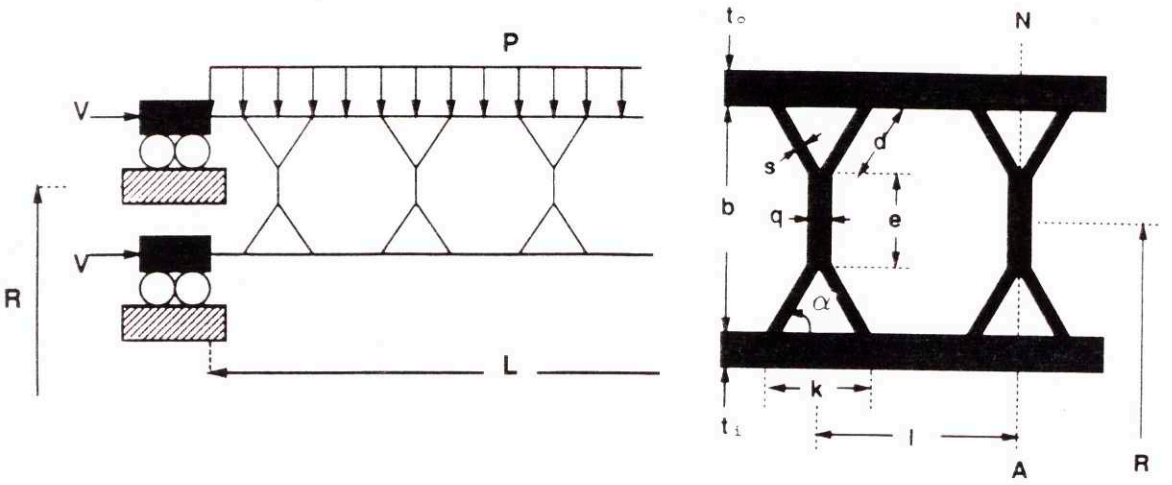

Fig. 1: A sandwich shell with double V-shaped core stiffeners

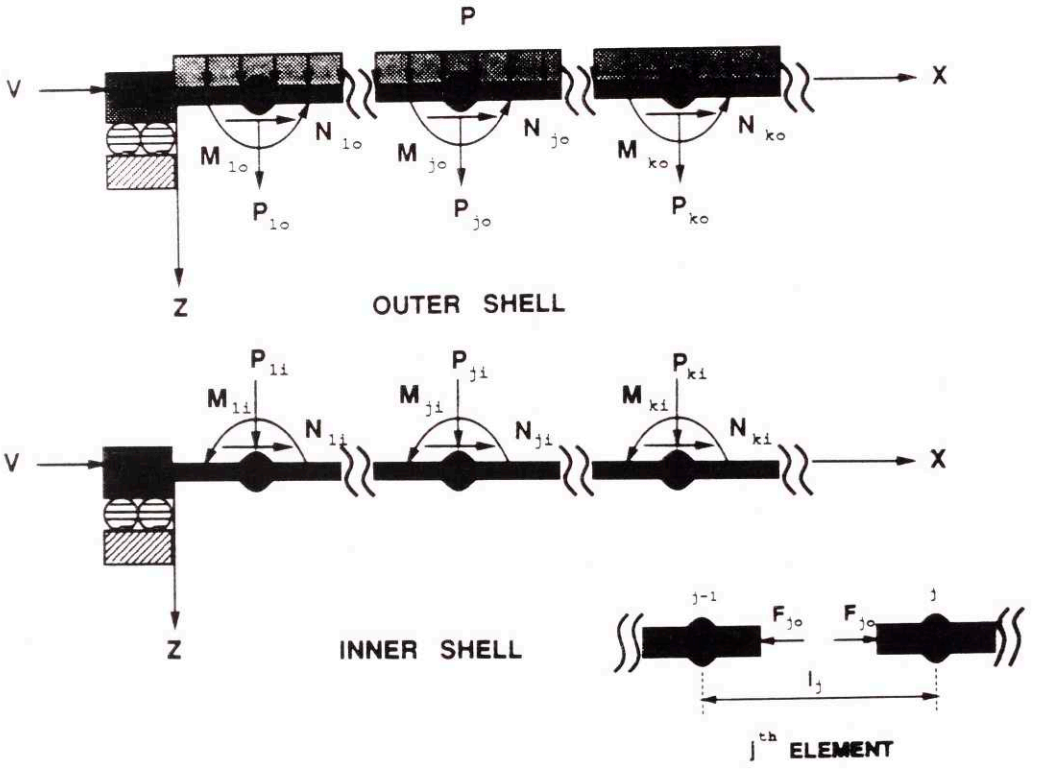

Fig. 2: Free body diagrams of the shells

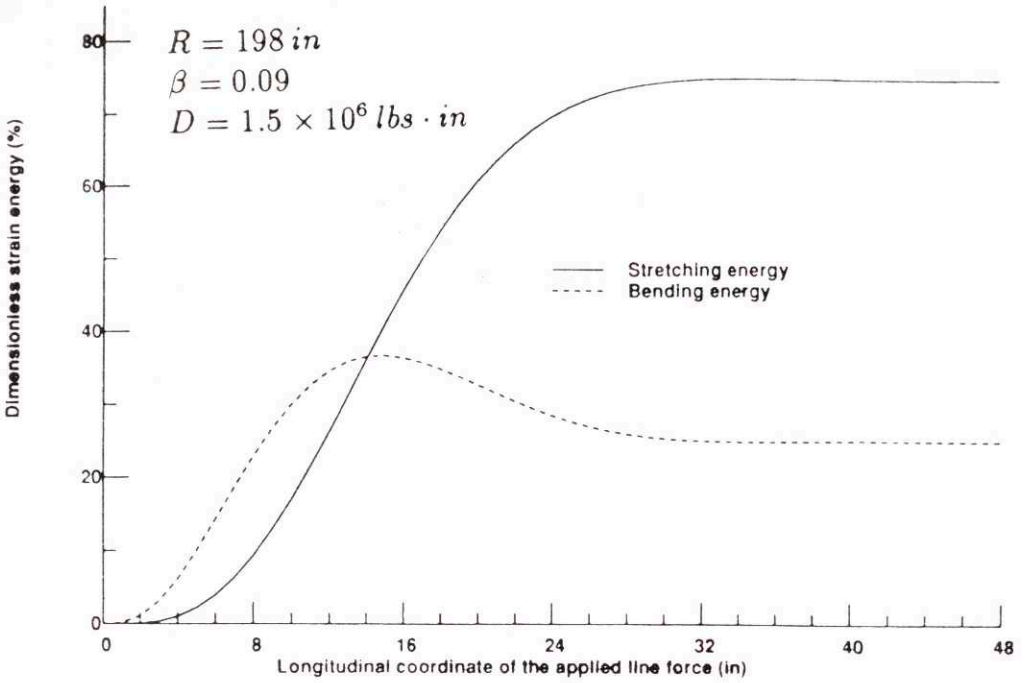

Fig. 3: Stretching and bending energy due to a unit line force

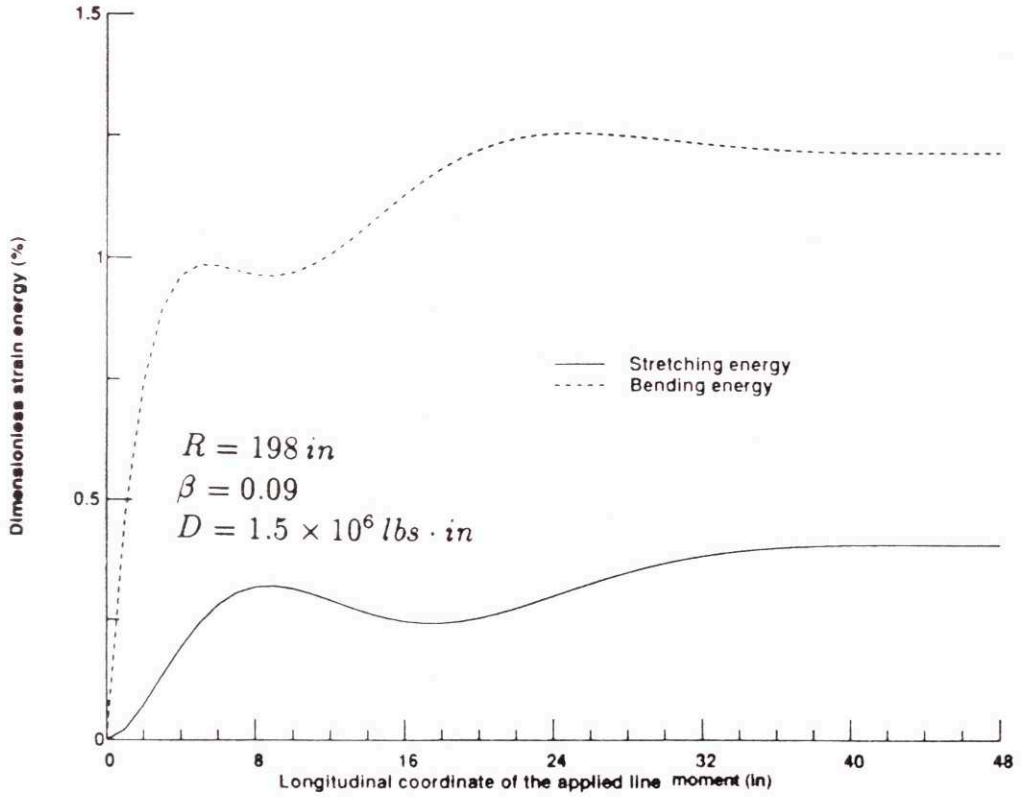

Fig. 4: Stretching and bending energy due to a unit line moment

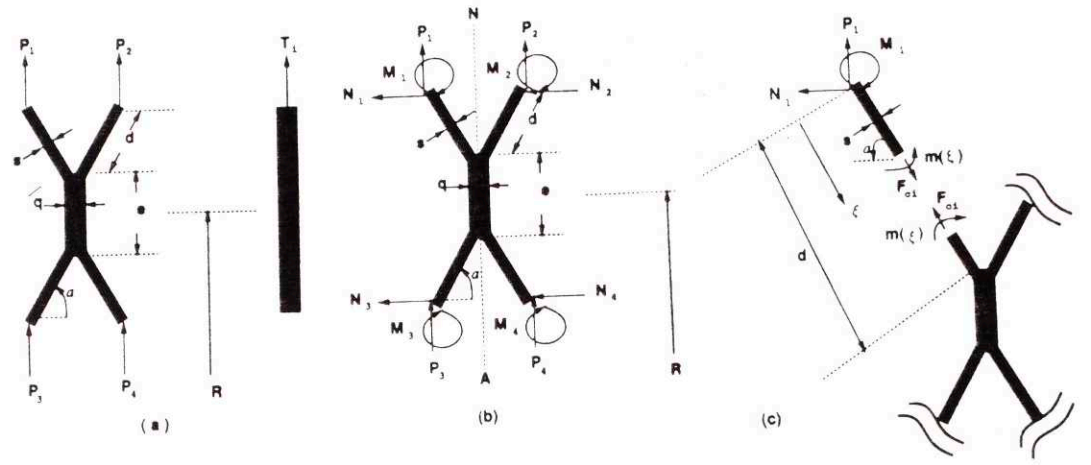

Fig. 5: Equivalent cross section and free body diagrams of the core stiffener

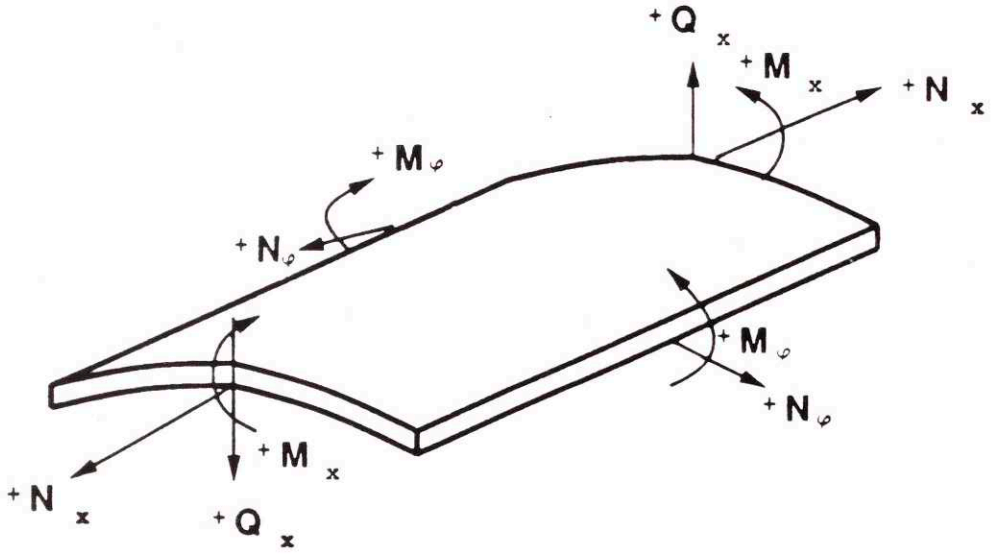

Fig. 6: Notation and sign convention

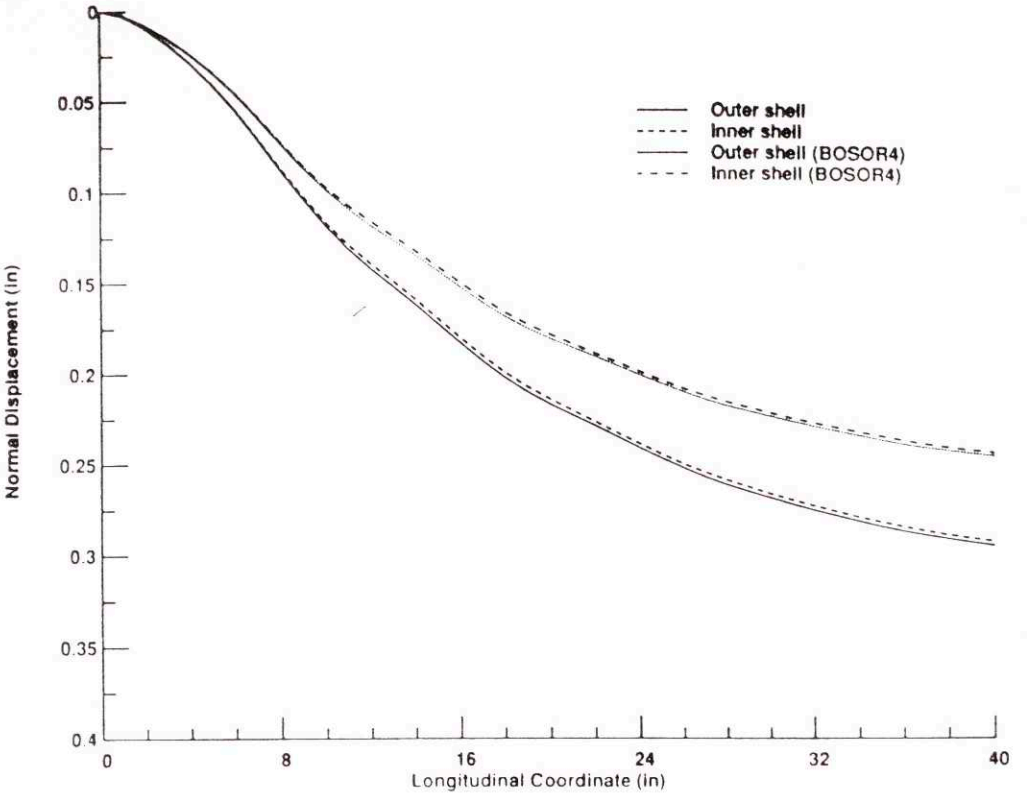

Fig. 7: Normal displacement diagram of the sandwich shell

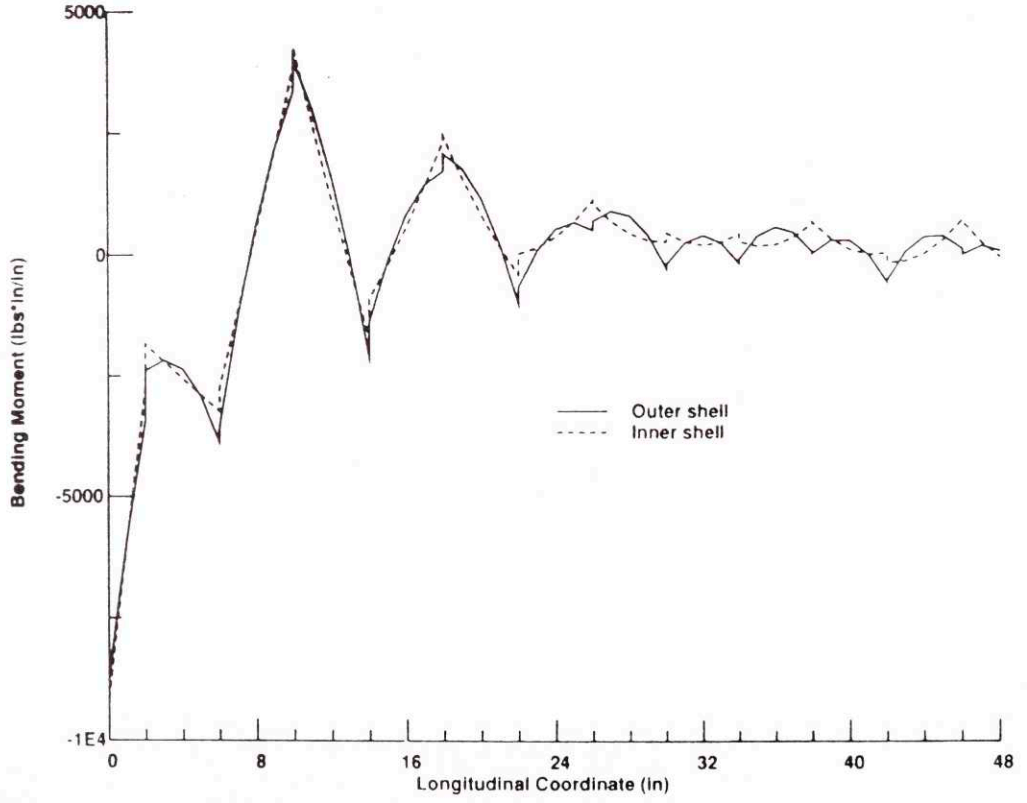

Fig. 8: Longitudinal bending moment diagram of the sandwich shell

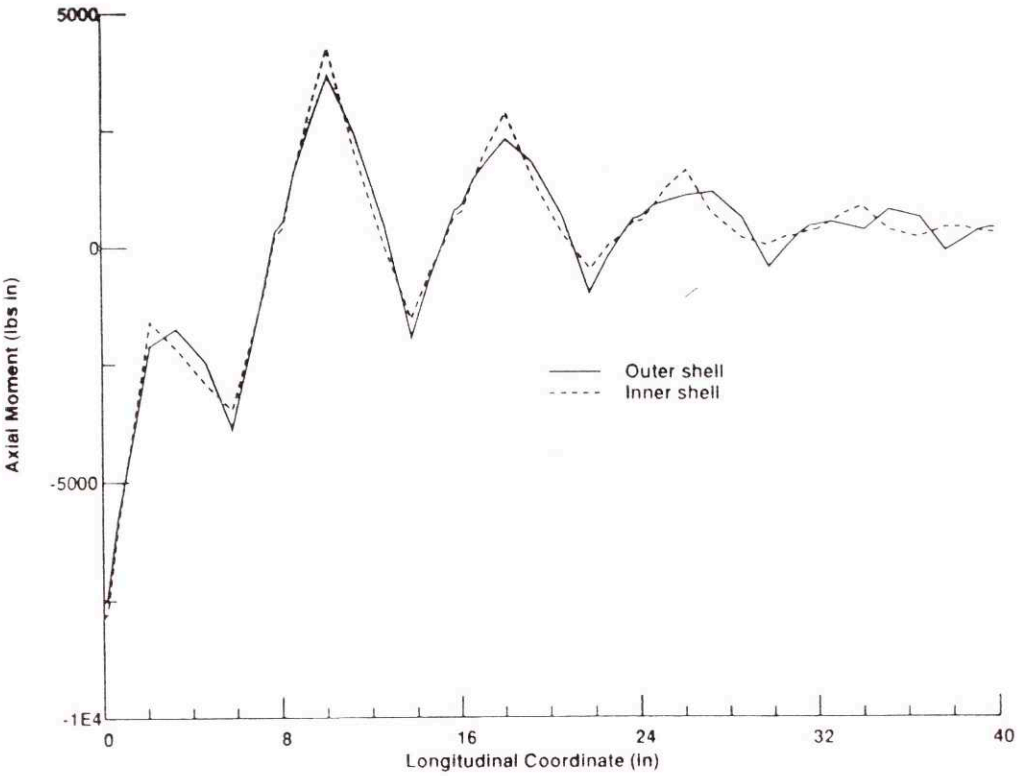

Fig. 9: Longitudinal bending moment ($BOSOR4$)

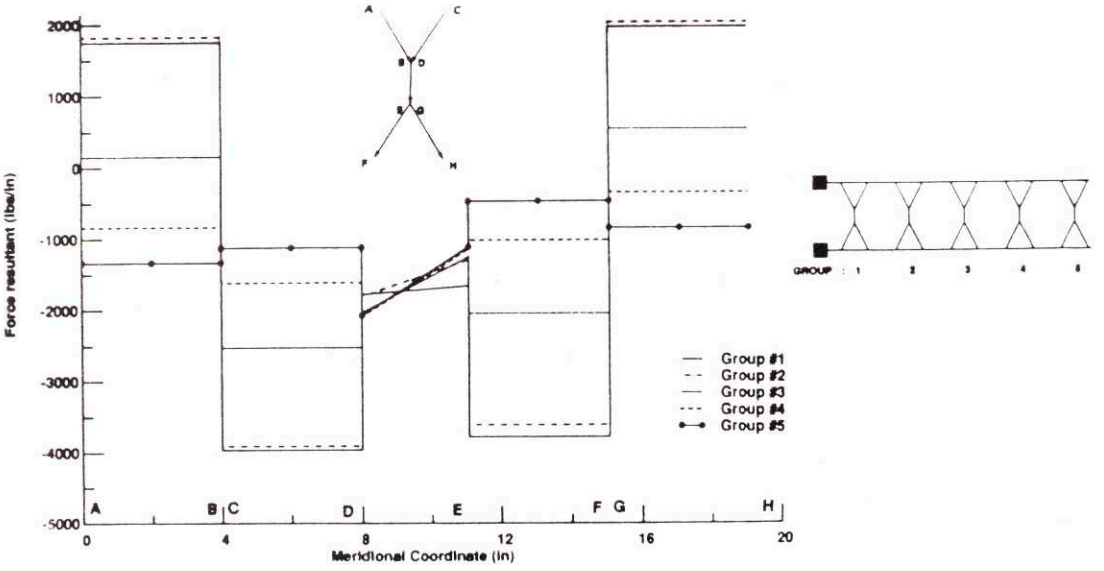

Fig. 10: Force resultants along the meridian of the core stiffeners

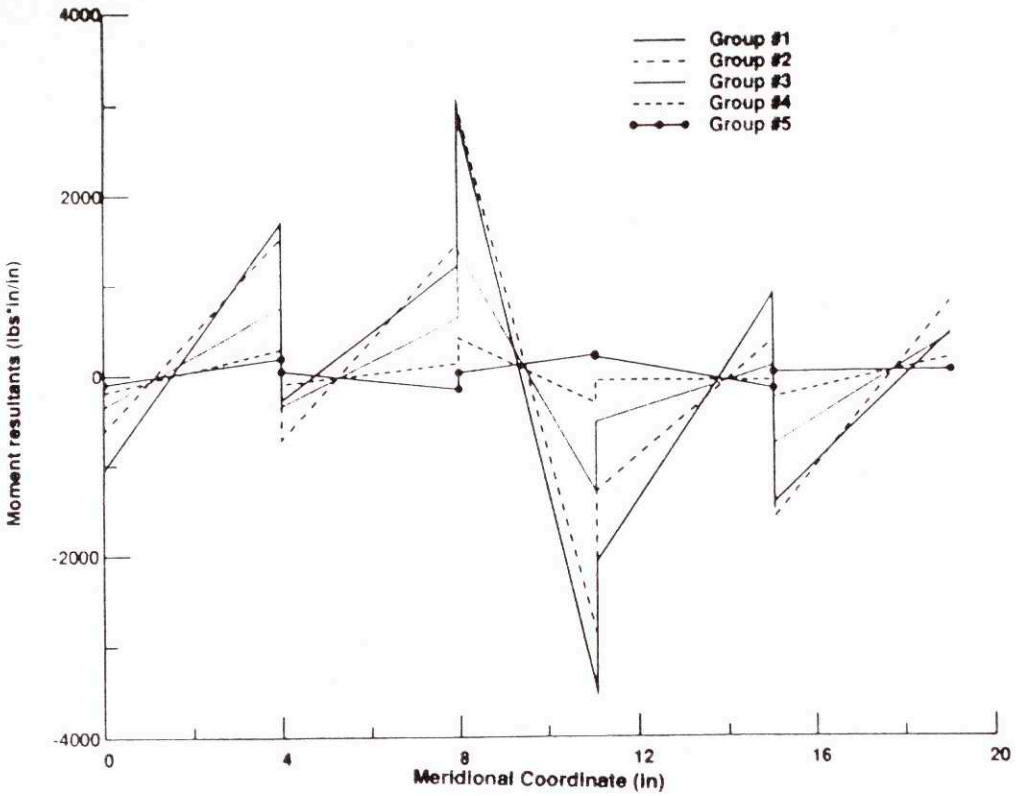

Fig. 11: Moment resultants along the meridian of the core stiffeners

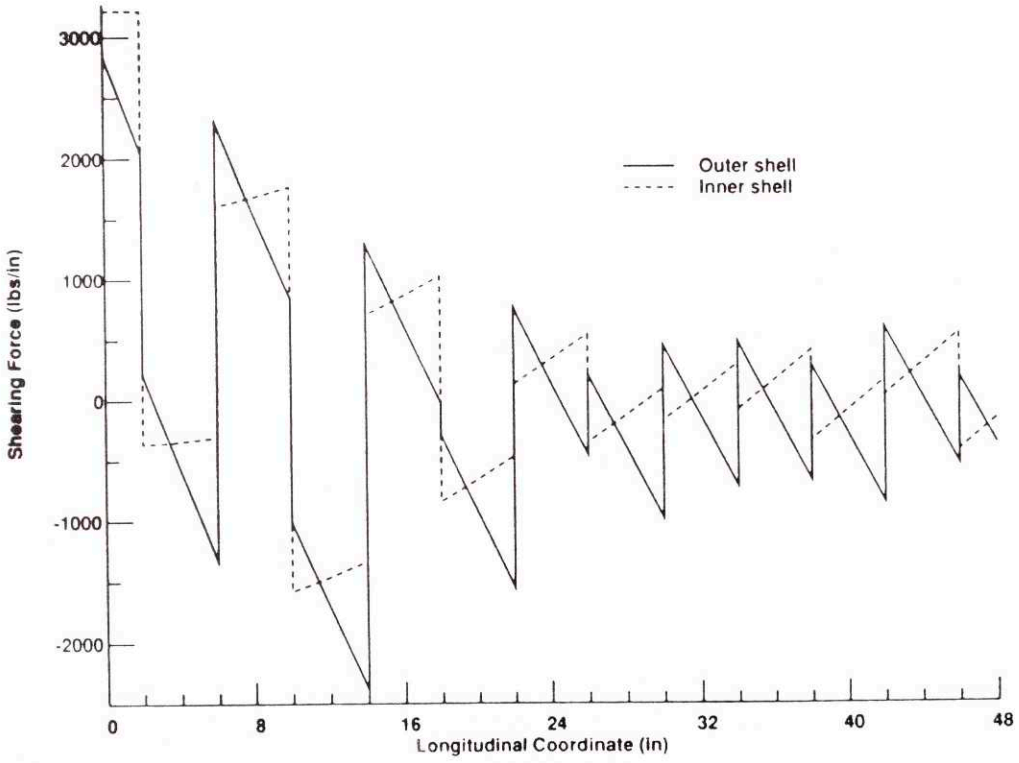

Fig. 12: Transverse shearing force diagram of the sandwich shell

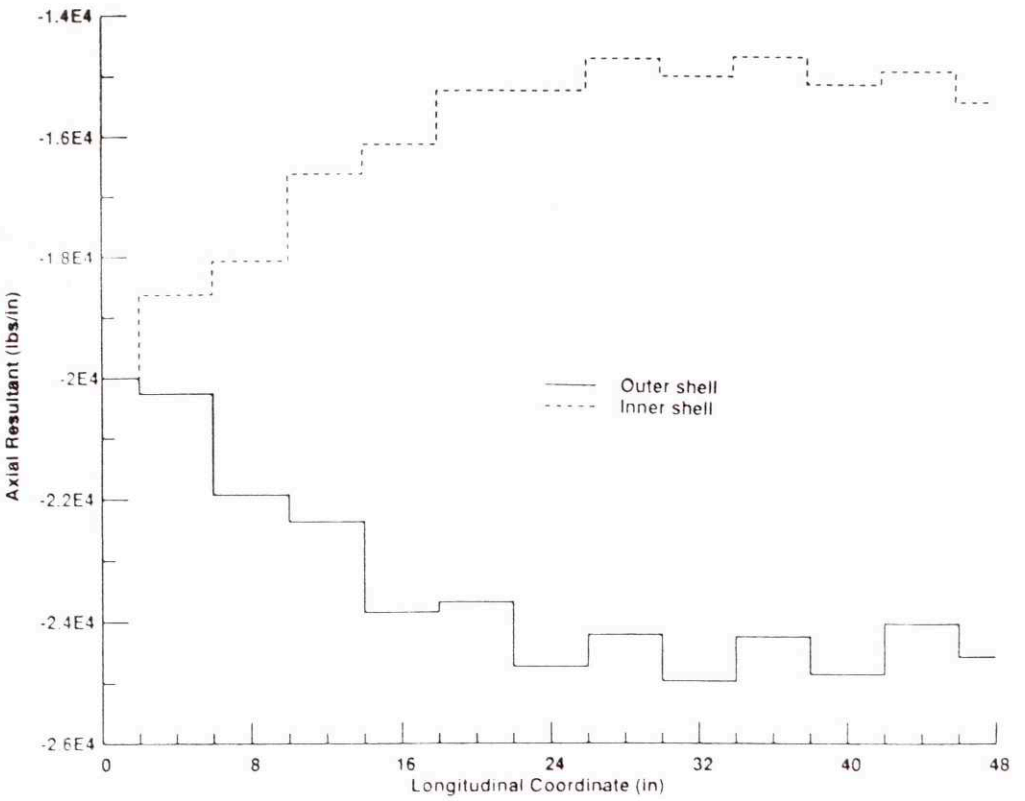

Fig. 13: Axial load distribution along the inner and outer shell

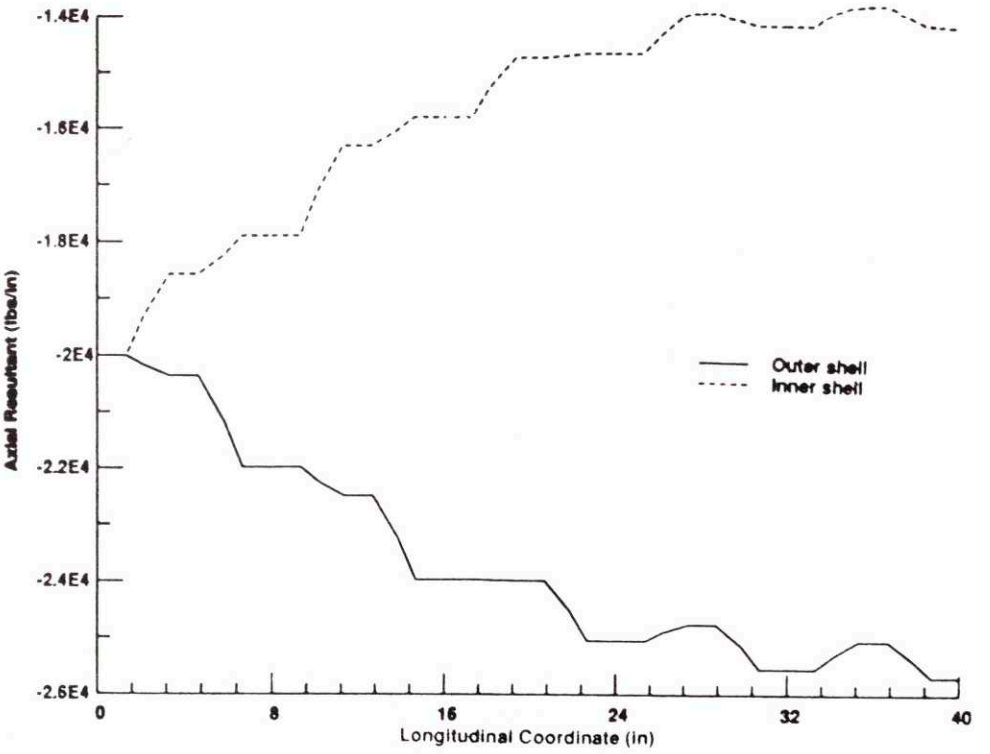

Fig. 14: Axial load distribution ($BOSOR4$)

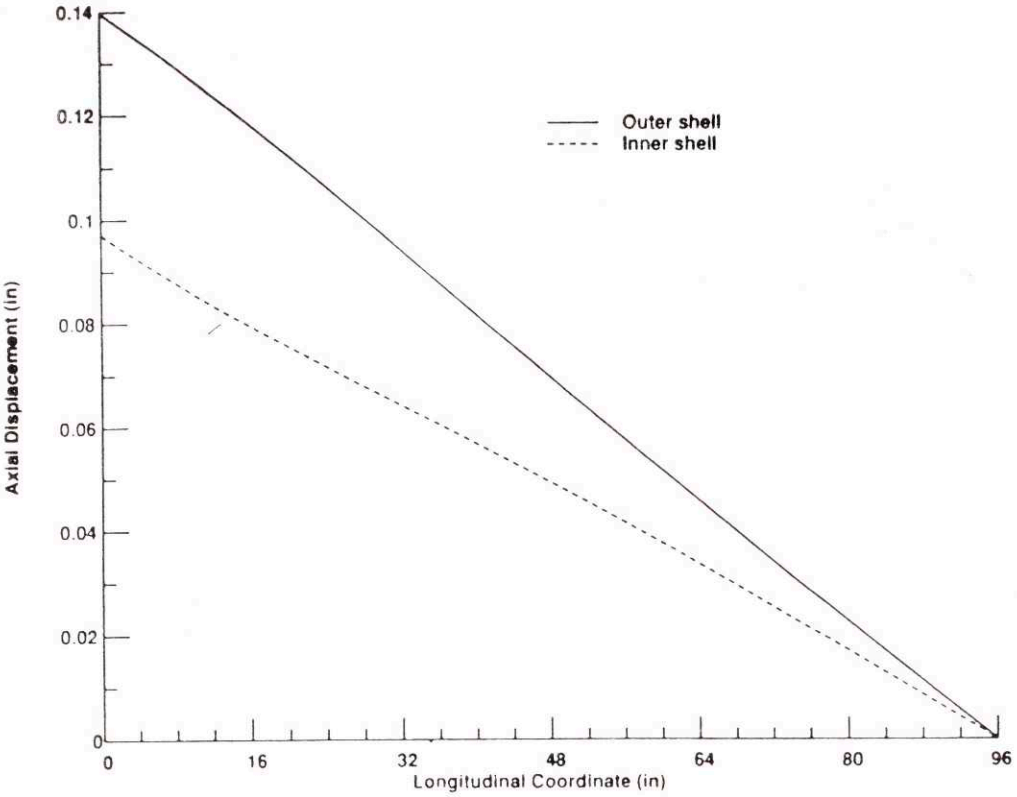

Fig. 15: Axial displacement diagram of the sandwich shell

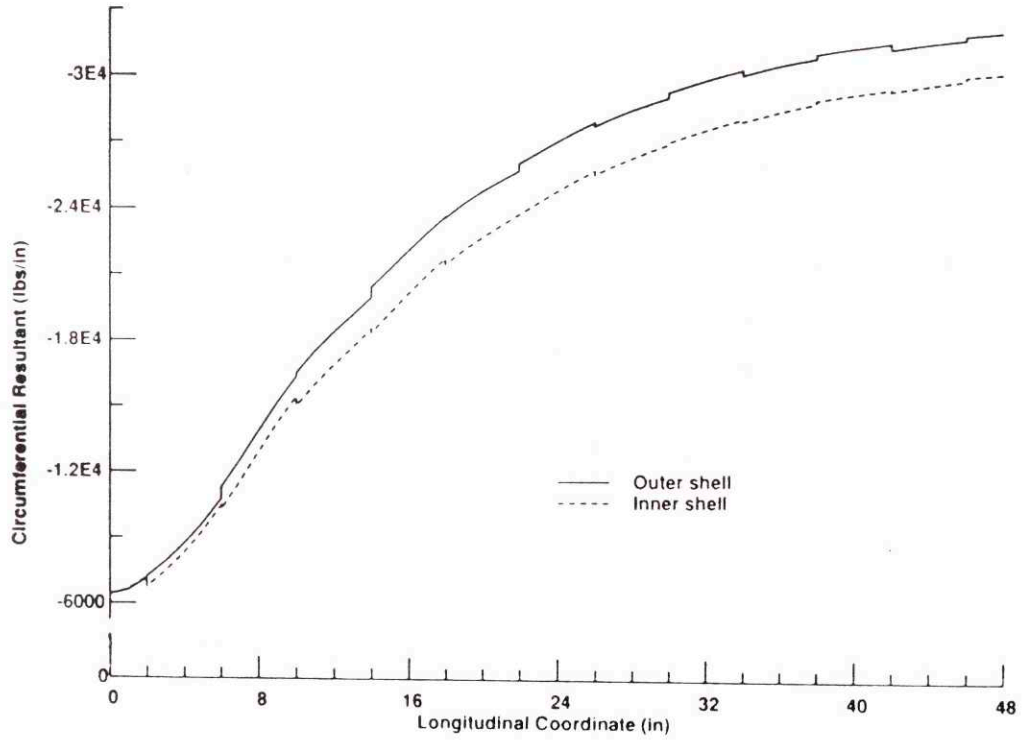

Fig. 16: Circumferential force resultant of the sandwich shell

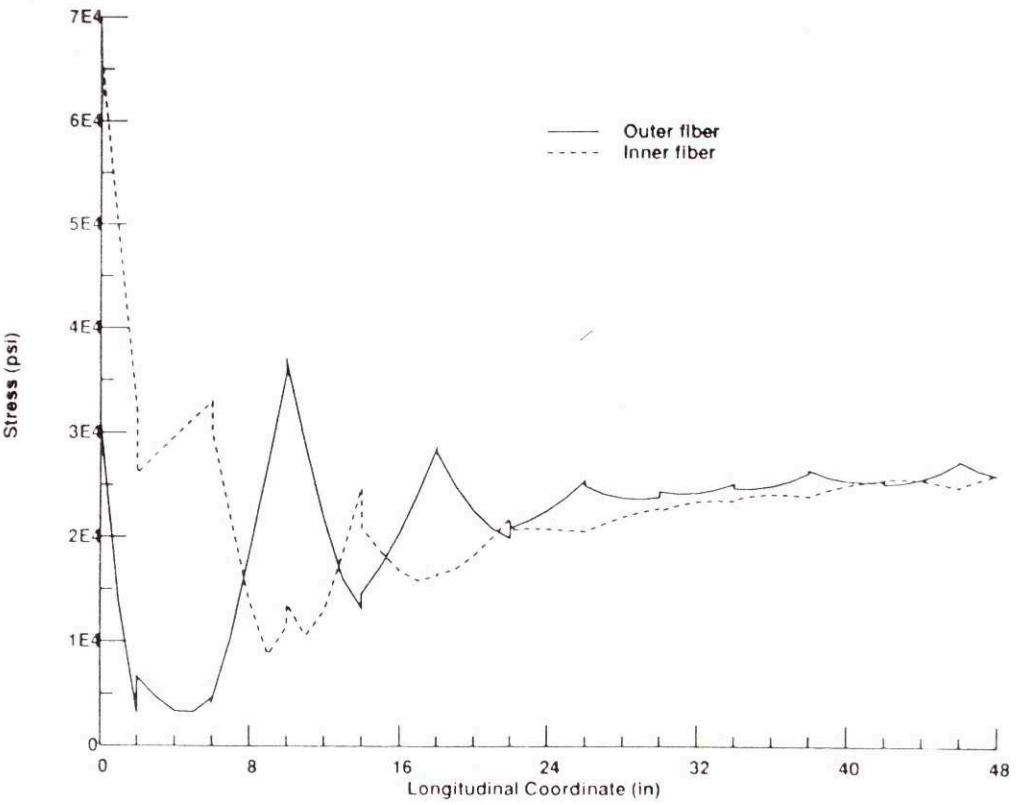

Fig. 17: Inner shell - Equivalent von Mises stress

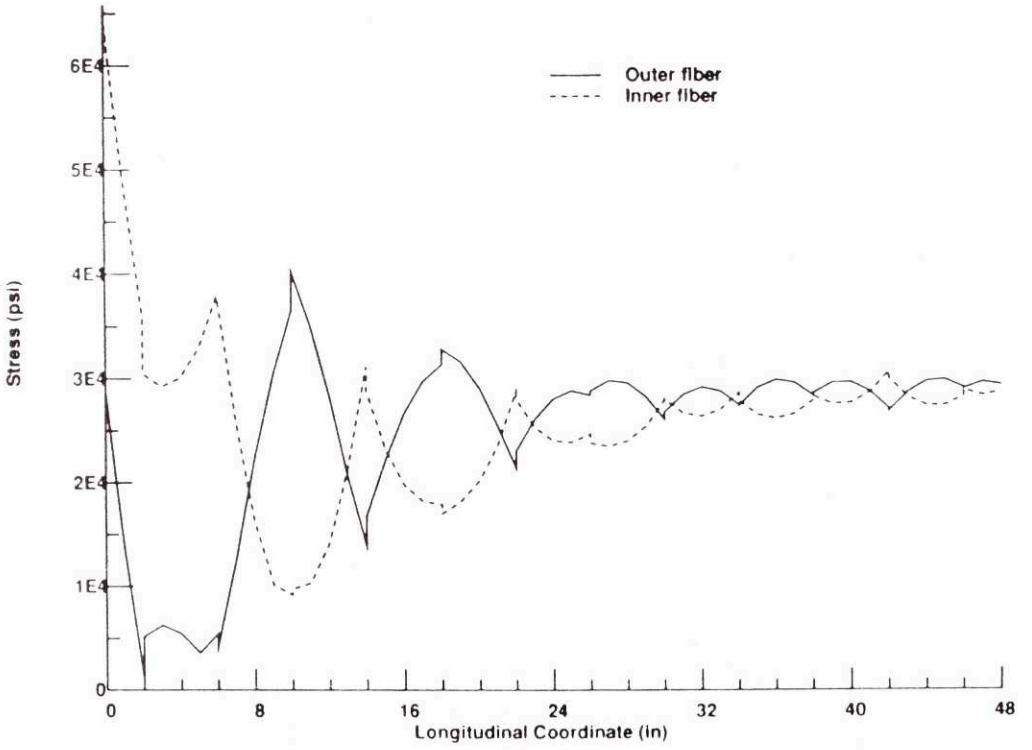

Fig. 18: Outer shell - Equivalent von Mises stress

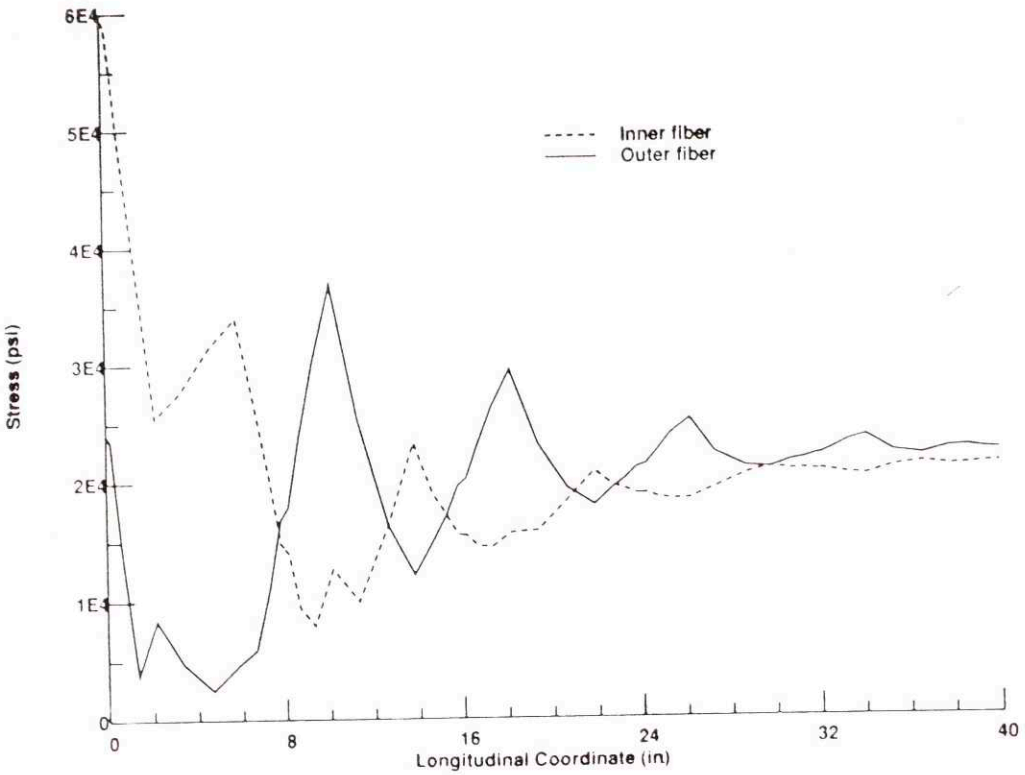

Fig. 19: Inner shell - Equivalent von Mises stress ($BOSOR4$)

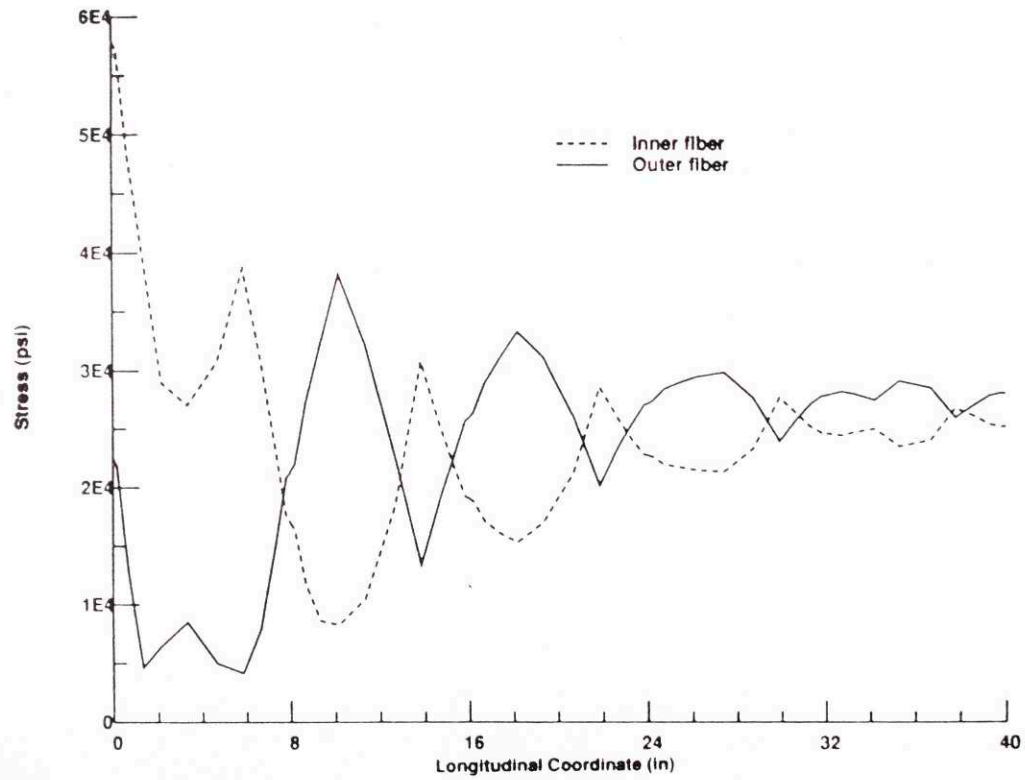

Fig. 20: Outer shell - Equivalent von Mises stress ($BOSOR4$)

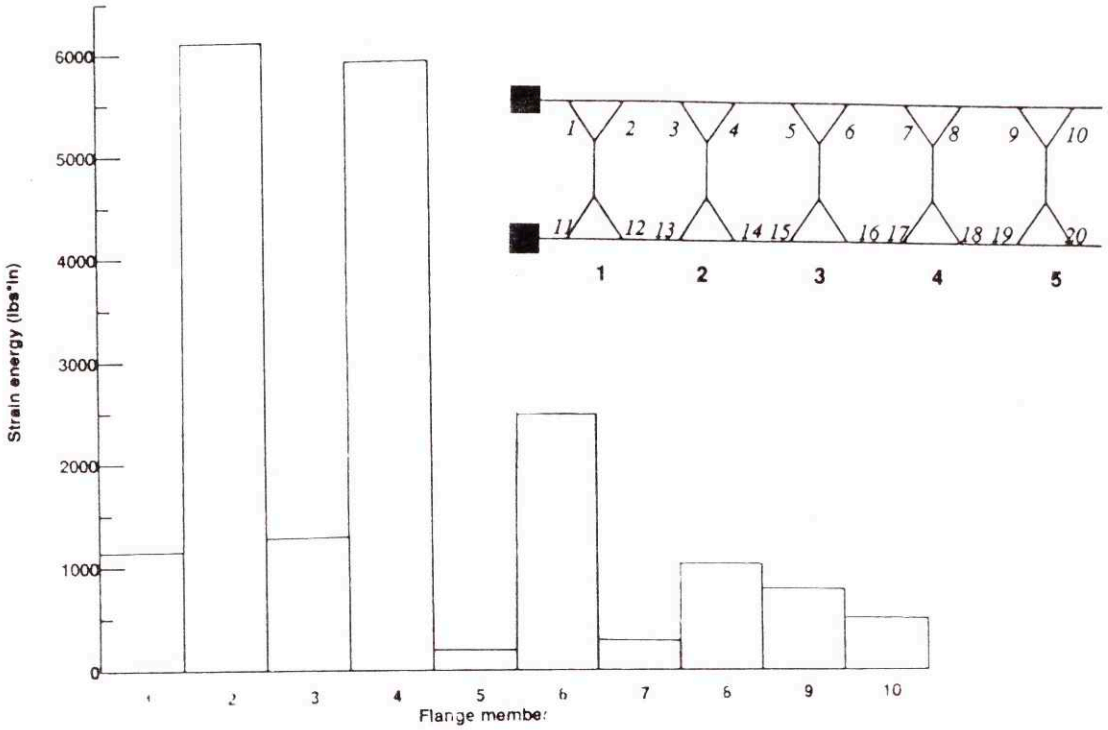

Fig. 21: Strain energy of the flanges due to local stretching

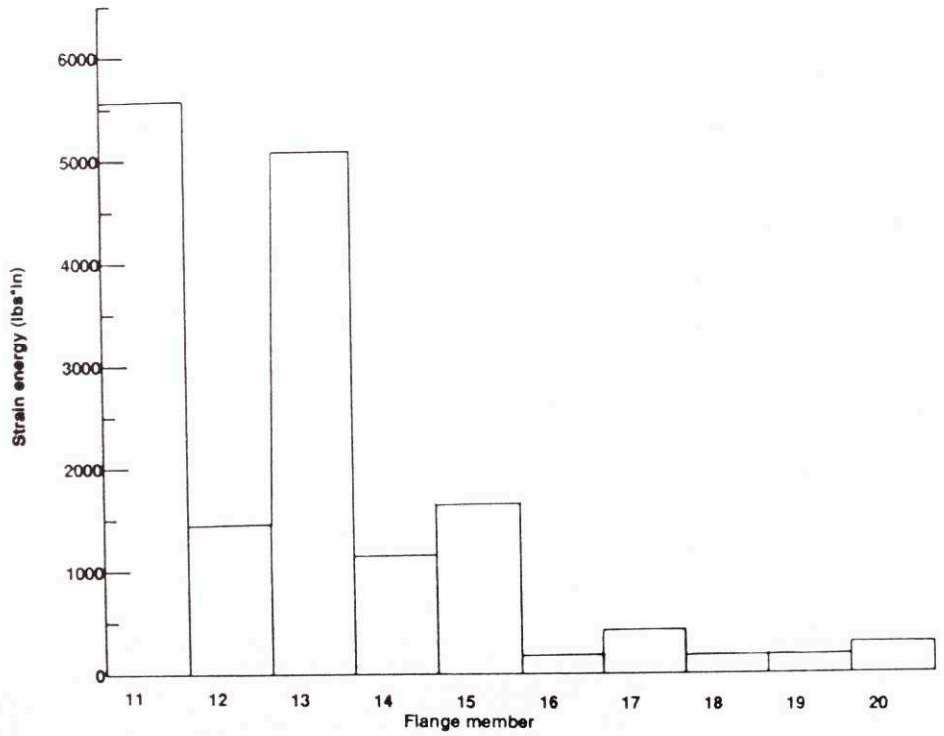

Fig. 22: Strain energy of the flanges due to local stretching

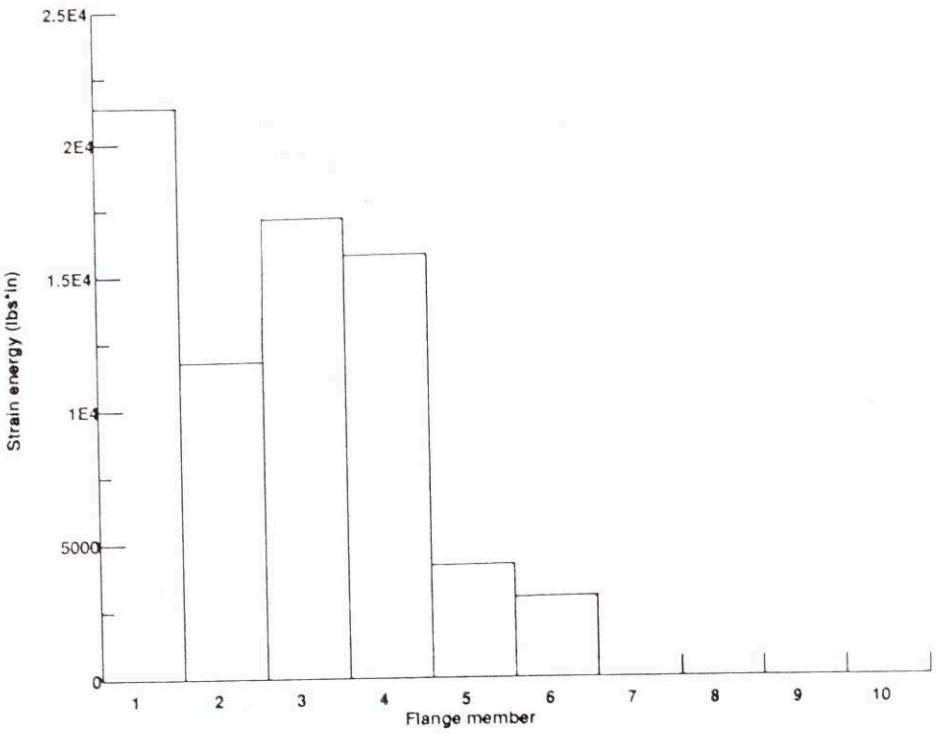

Fig. 23: Strain energy of the flanges due to local bending

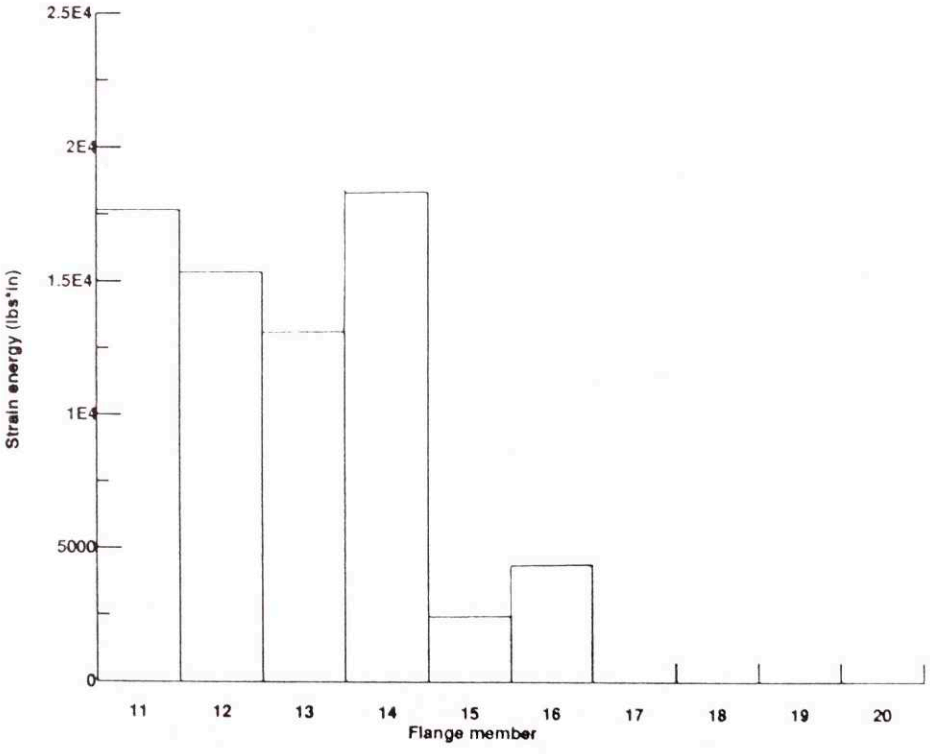

Fig. 24: Strain energy of the flanges due to local bending

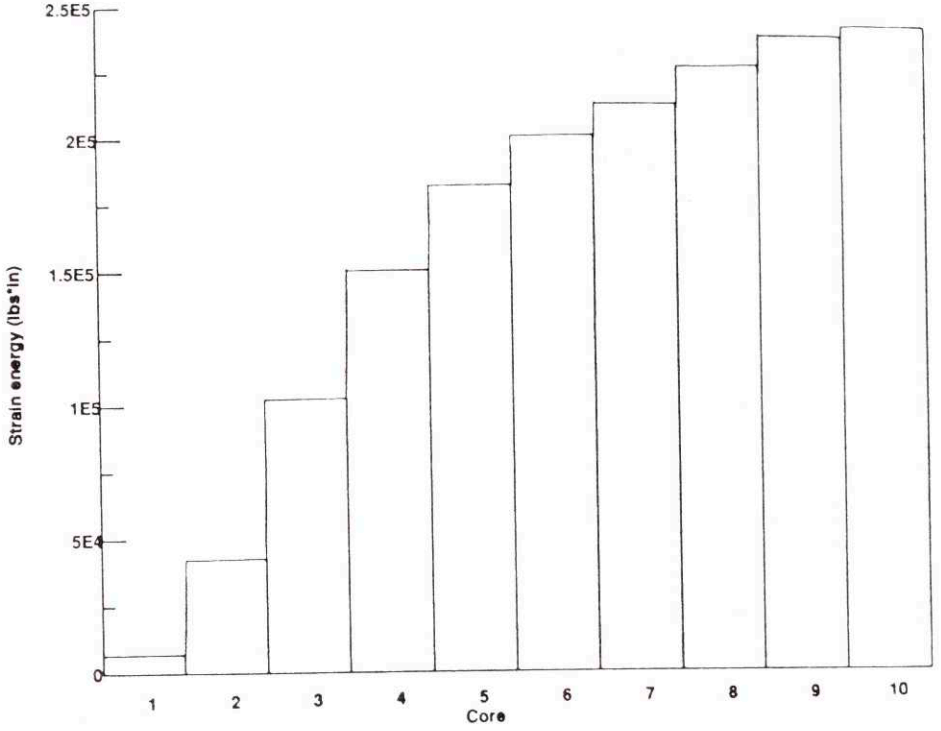

Fig. 25: Strain energy of the core stiffeners due to global stretching

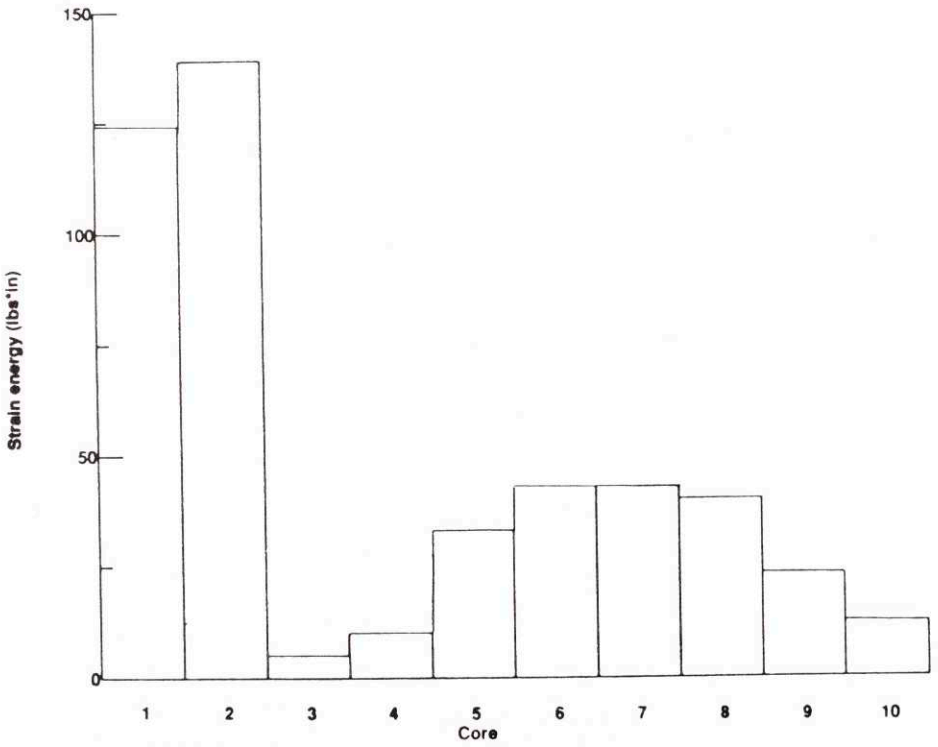

Fig. 26: Strain energy of the core stiffeners due to global twisting

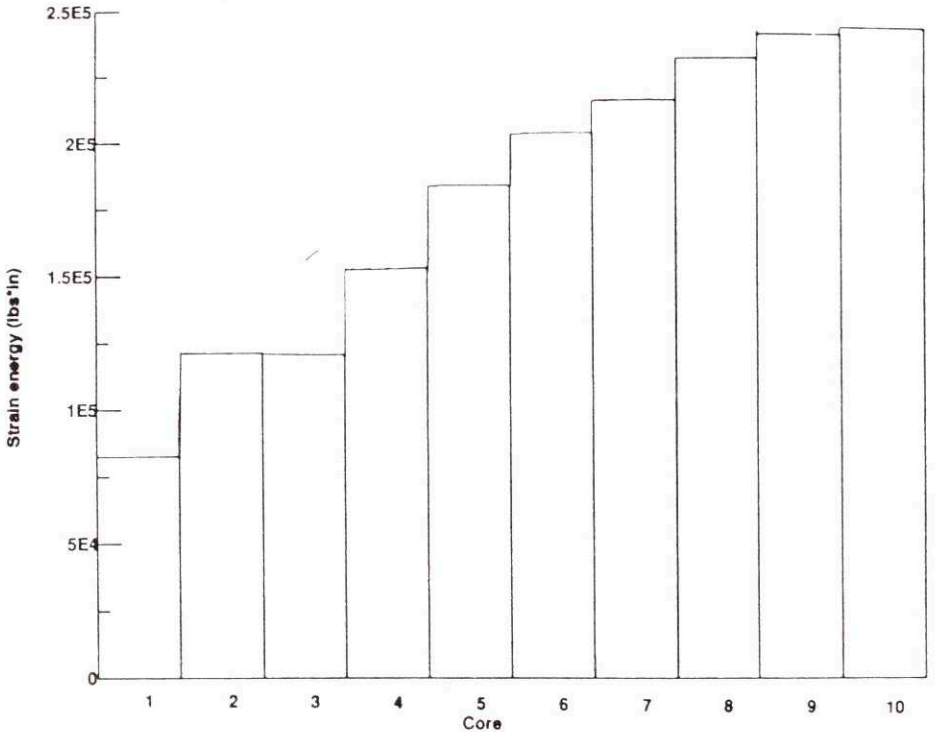

Fig. 27: Strain energy of the core stiffeners

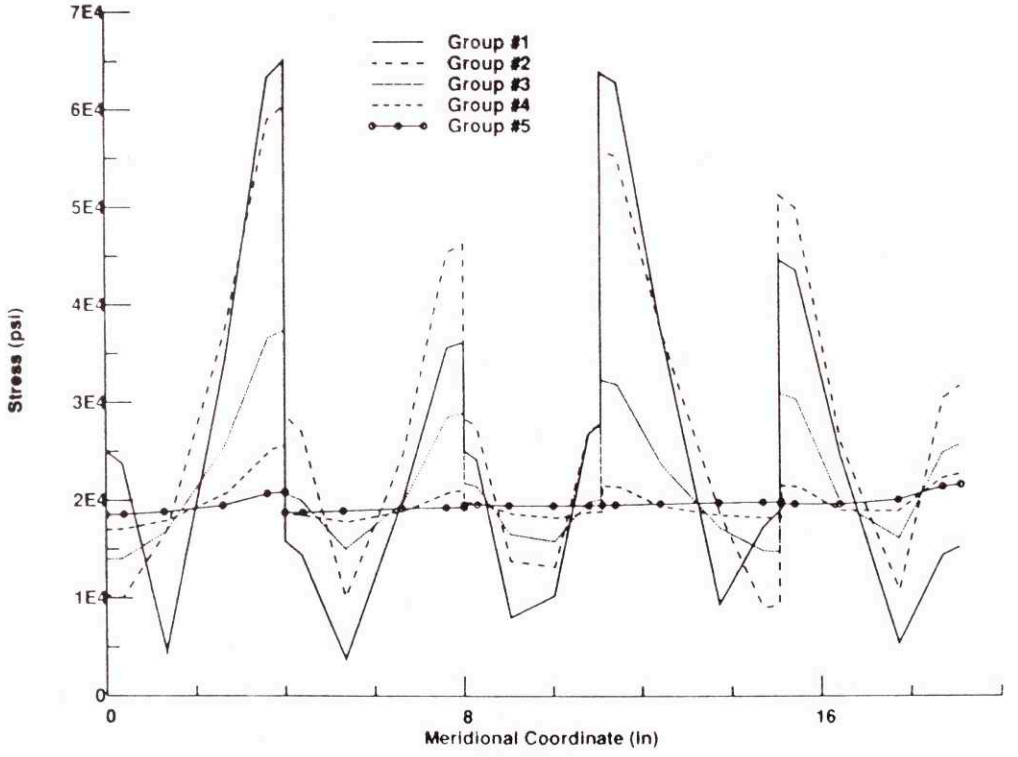

Fig. 28: Core stiffeners - Equivalent von Mises stress

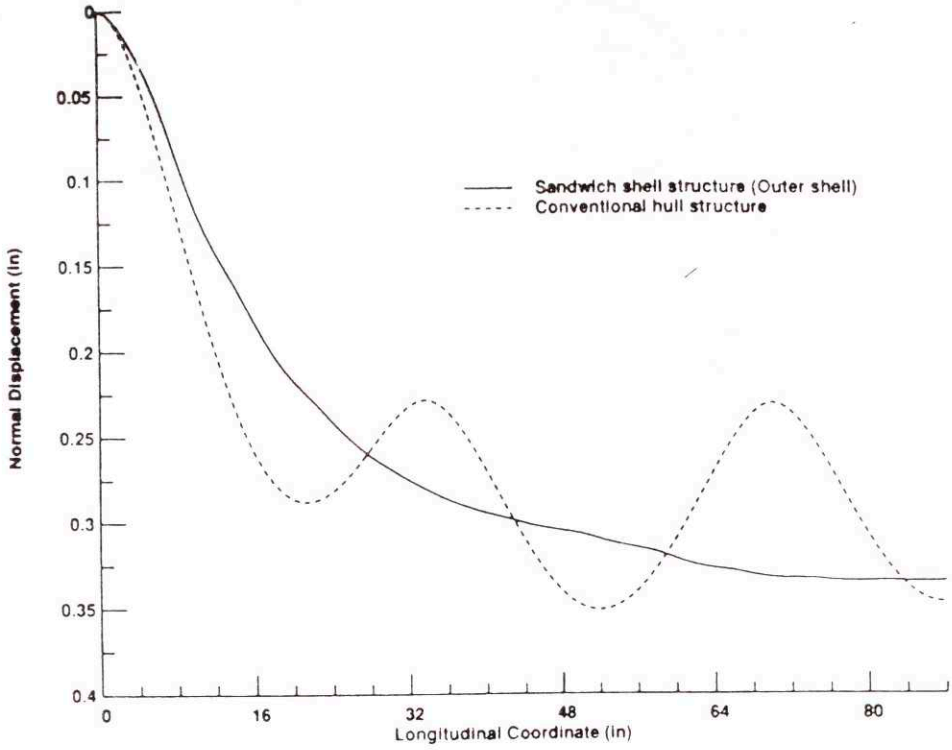

Fig. 29: Normal displacement diagram - Conventional vs sandwich shell

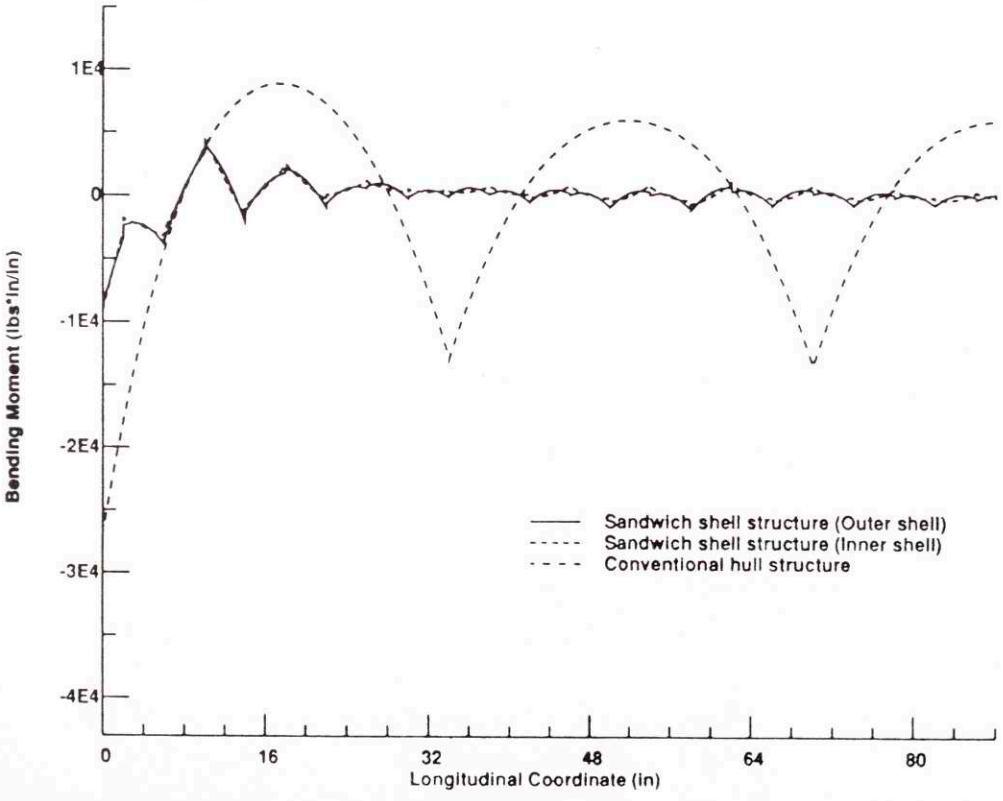

Fig. 30: Bending moment diagram - Conventional vs sandwich shell

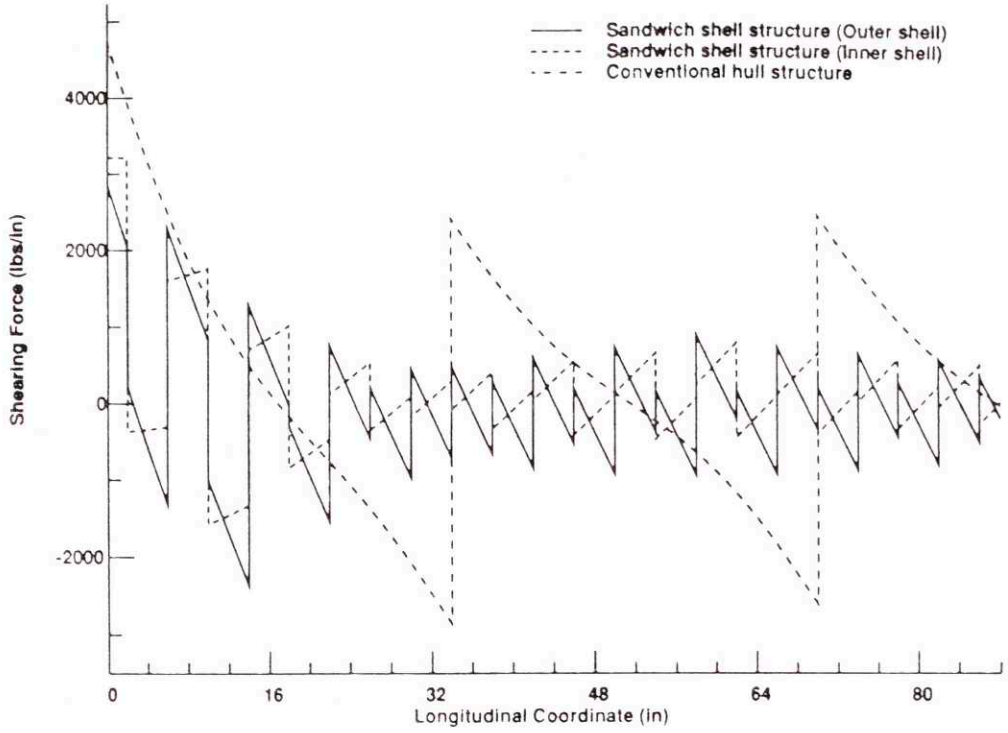

Fig. 31: Shearing force diagram - Conventional vs sandwich shell

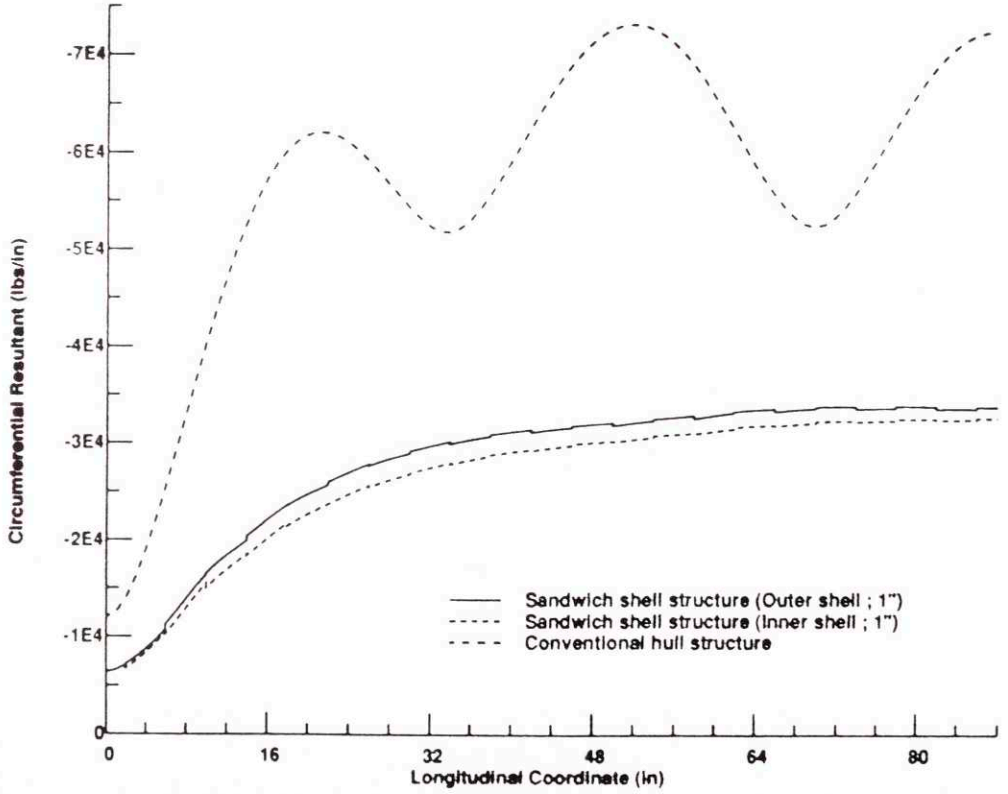

Fig. 32: Circumferential force resultant - Conventional vs sandwich shell

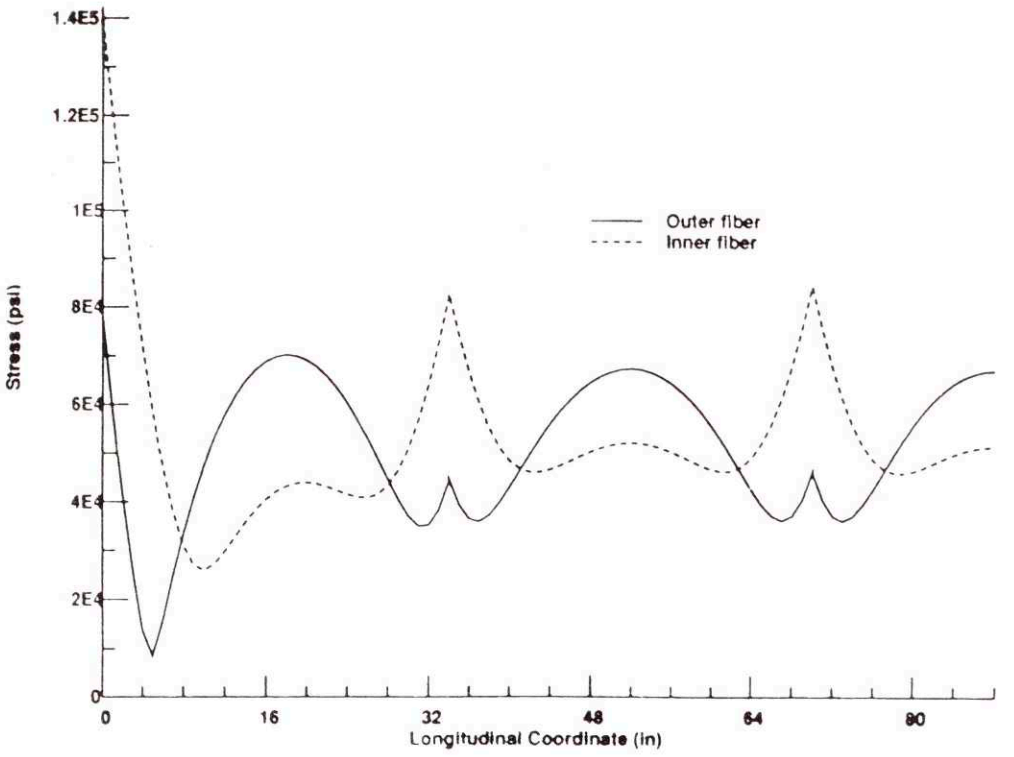

Fig. 33: Conventional hull - Equivalent von Mises stress

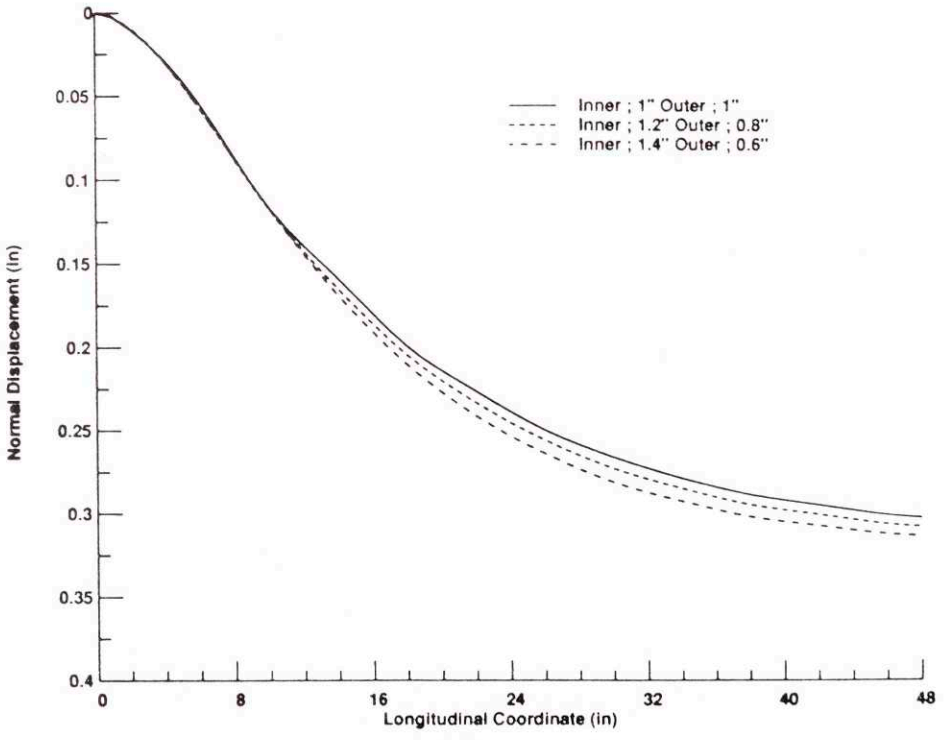

Fig. 34: Inner shell - Normal displacement diagram of the sandwich shell

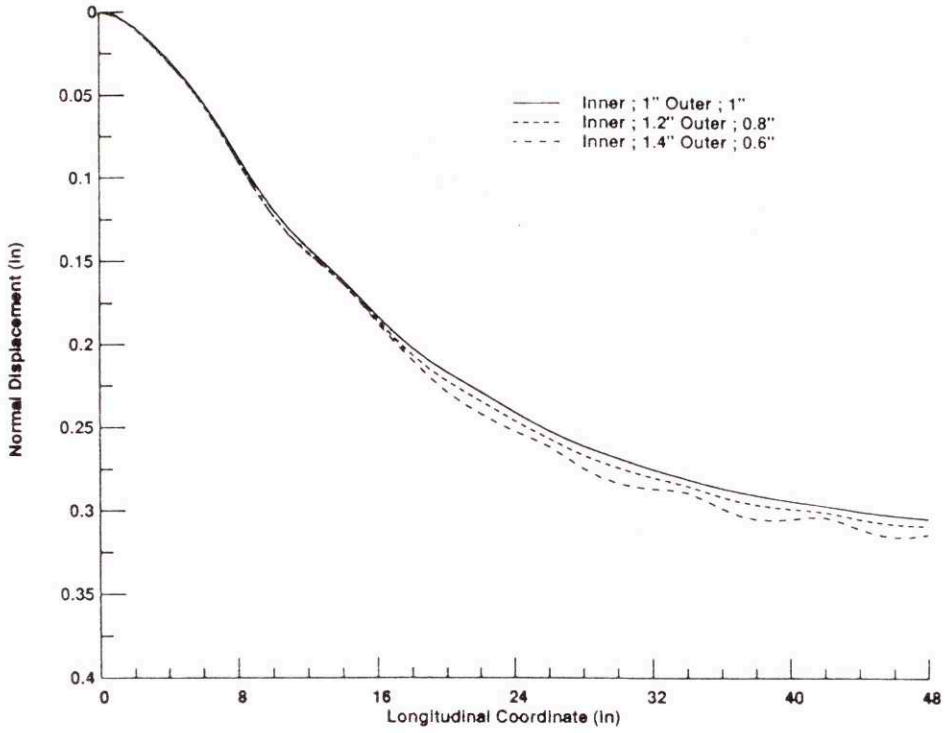

Fig. 35: Outer shell - Normal displacement diagram of the sandwich shell

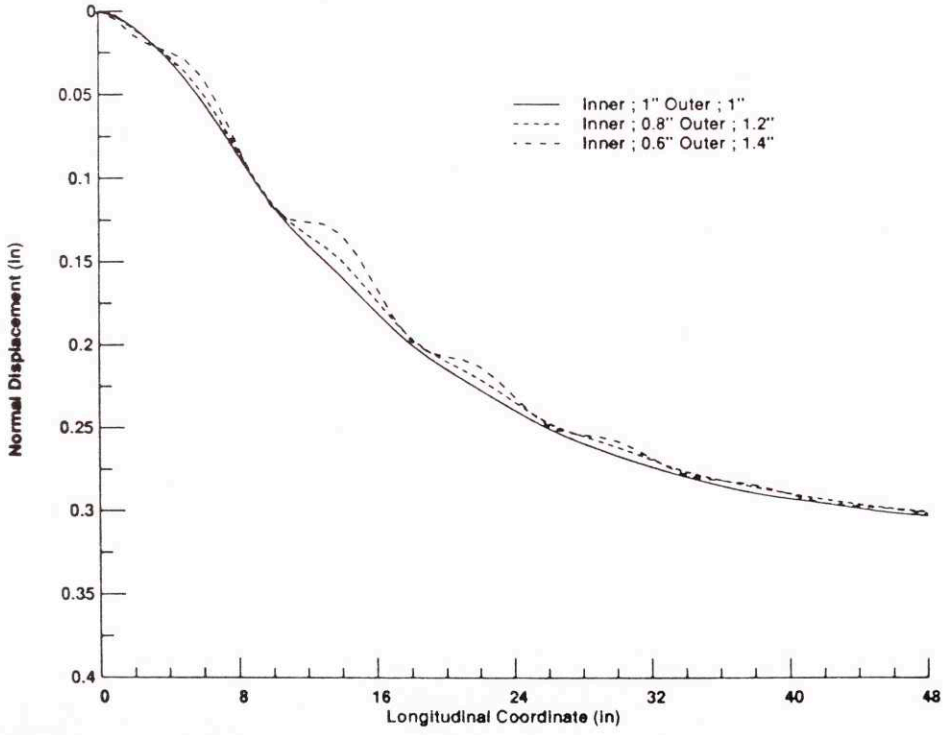

Fig. 36: Inner shell - Normal displacement diagram of the sandwich shell

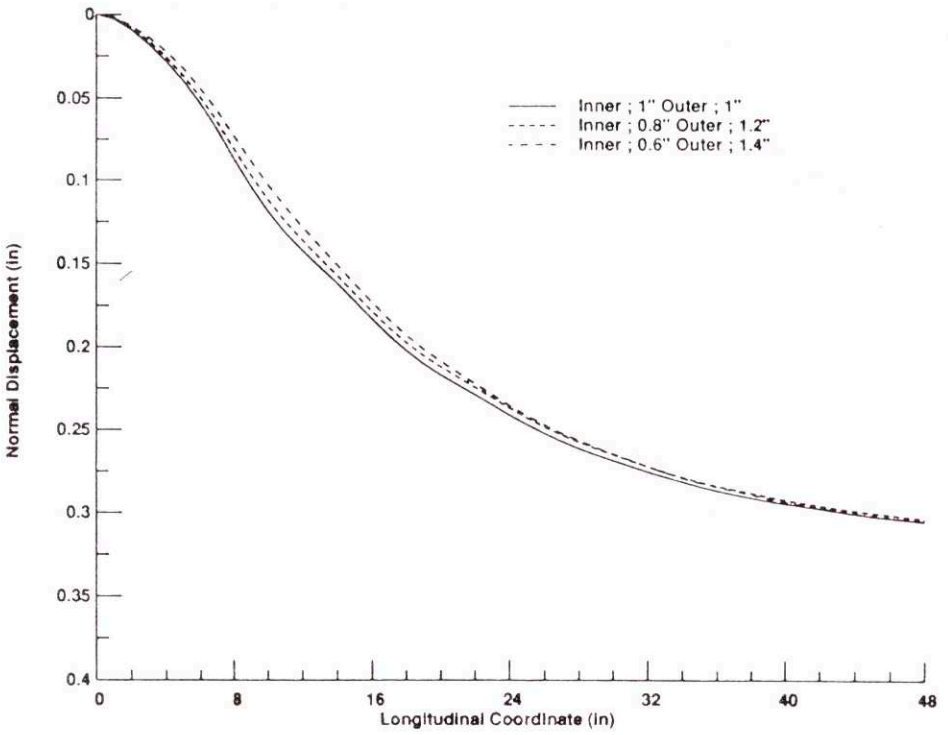

Fig. 37: Outer shell - Normal displacement diagram of the sandwich shell

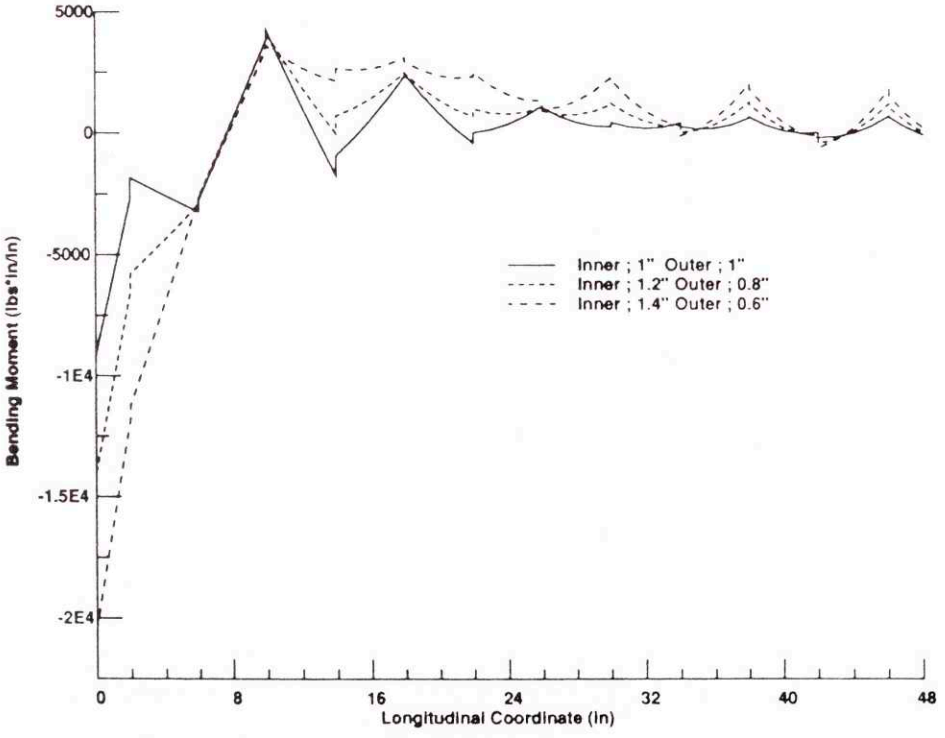

Fig. 38: Inner shell - Bending moment diagram of the sandwich shell

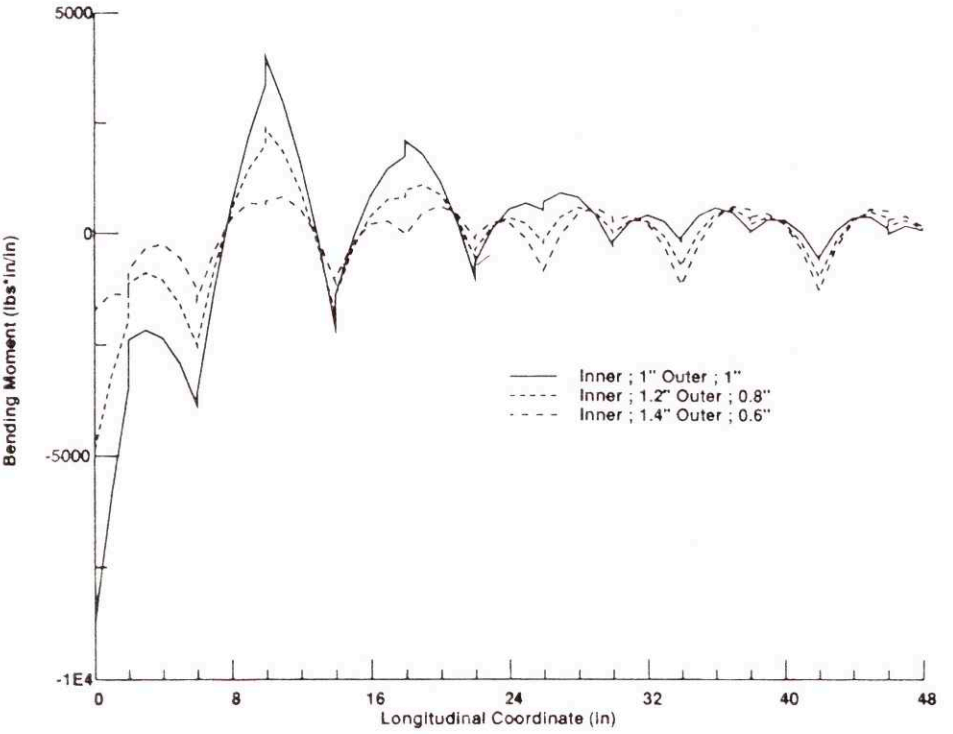

Fig. 39: Outer shell - Bending moment diagram of the sandwich shell

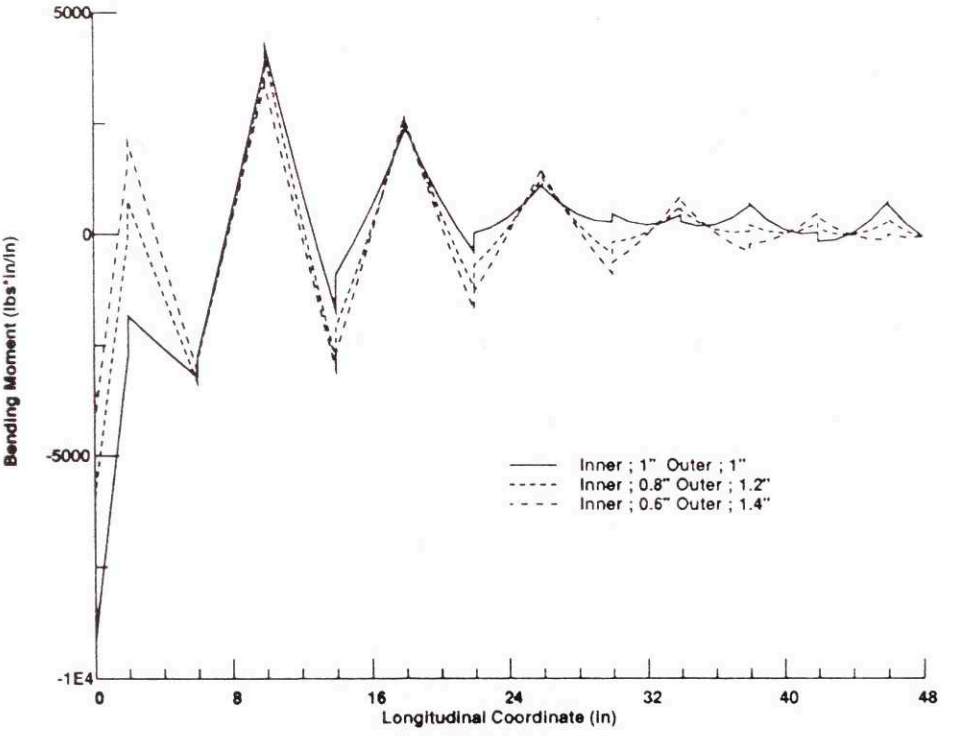

Fig. 40: Inner shell - Bending moment diagram of the sandwich shell

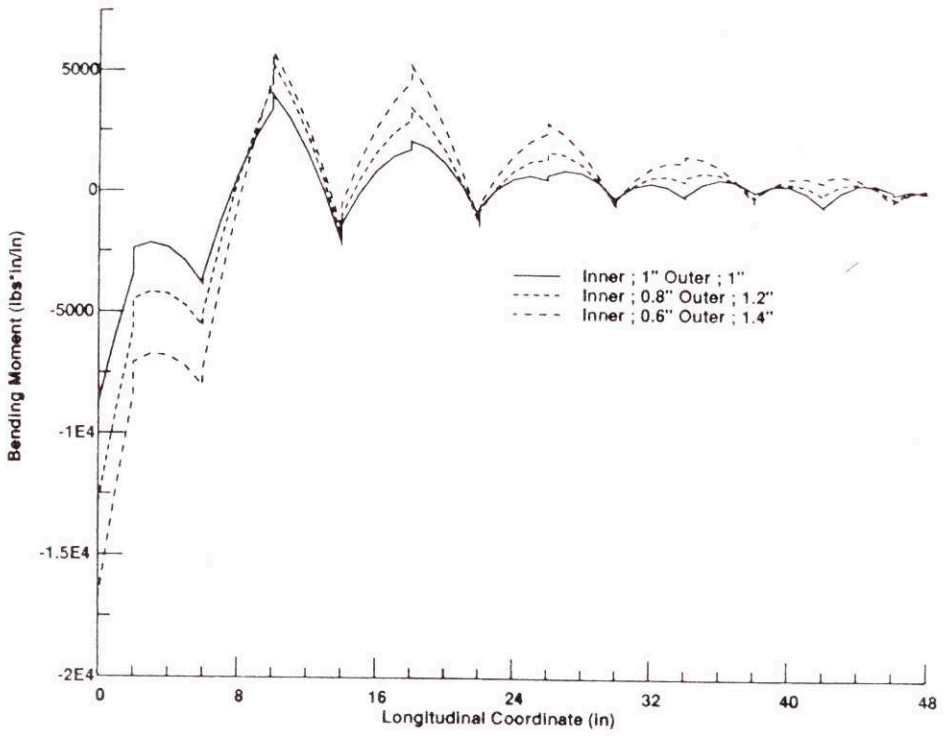

Fig. 41: Outer shell - Bending moment diagram of the sandwich shell

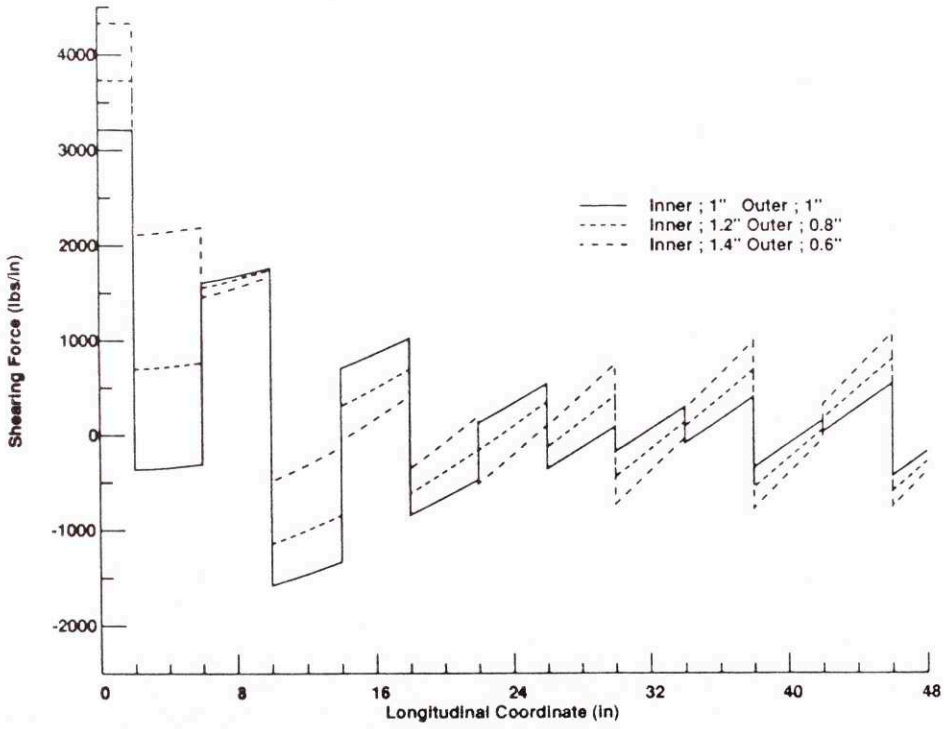

Fig. 42: Inner shell - Shearing force diagram of the sandwich shell

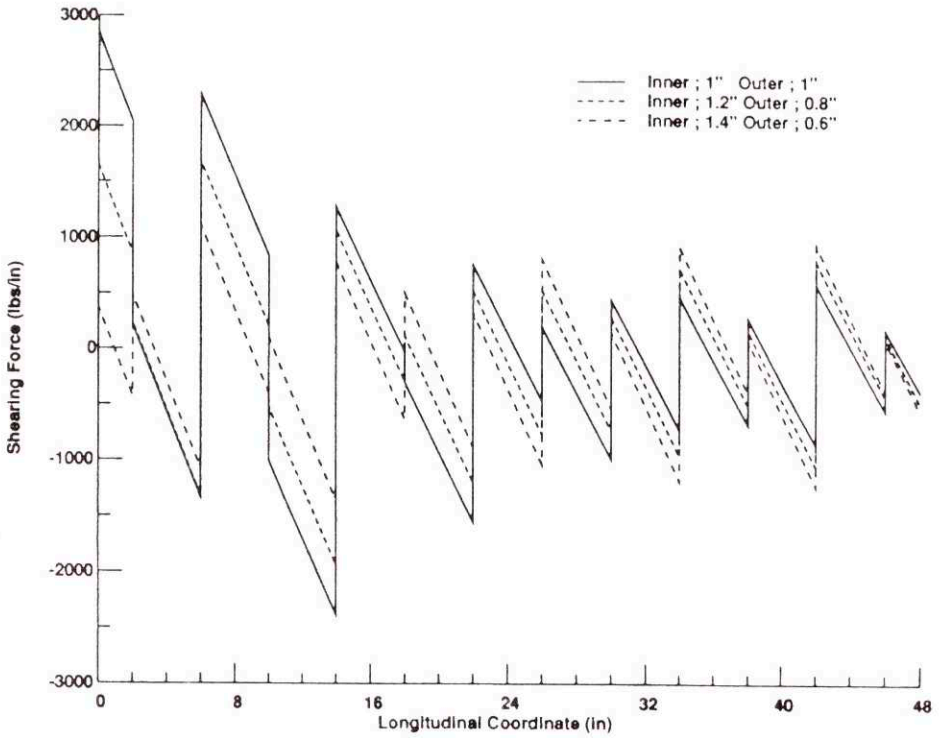

Fig. 43: Outer shell - Shearing force diagram of the sandwich shell

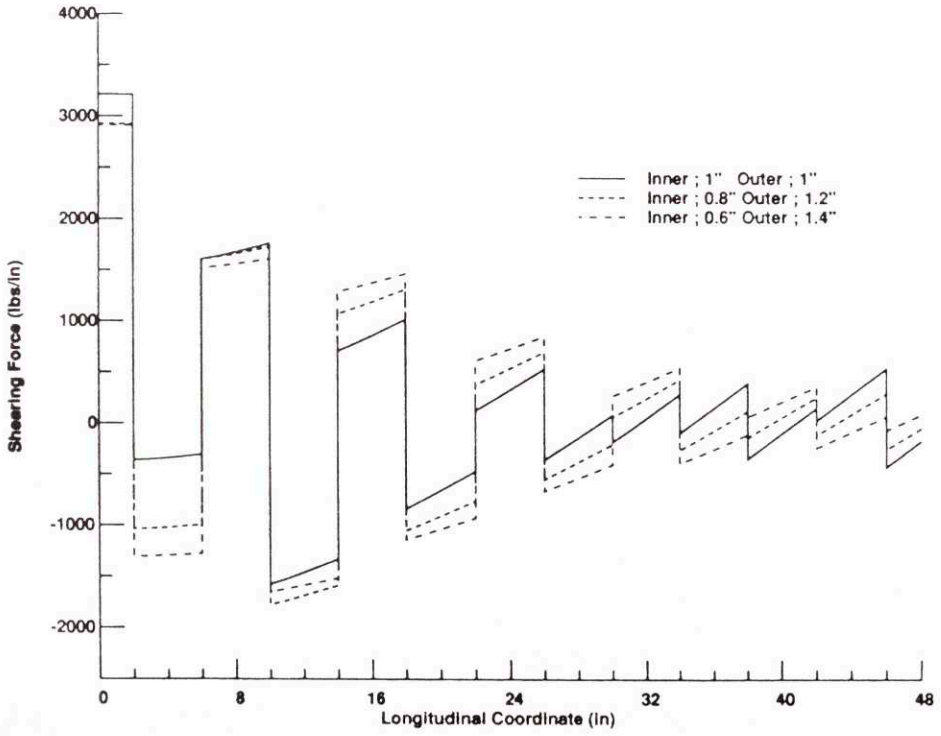

Fig. 44: Inner shell - Shearing force diagram of the sandwich shell

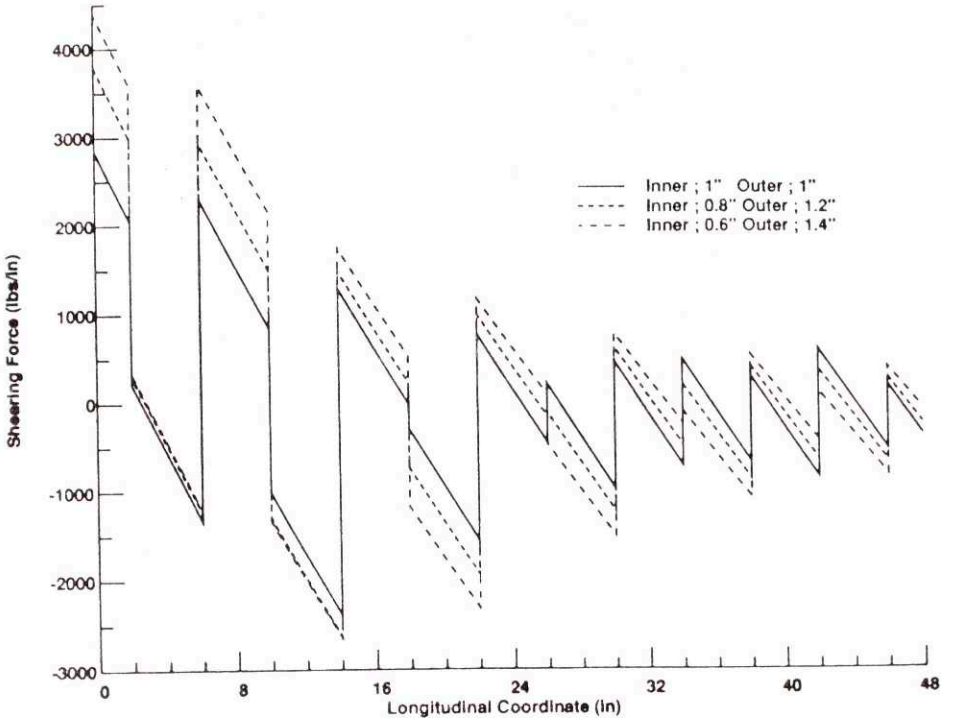

Fig. 45: Outer shell - Shearing force diagram of the sandwich shell

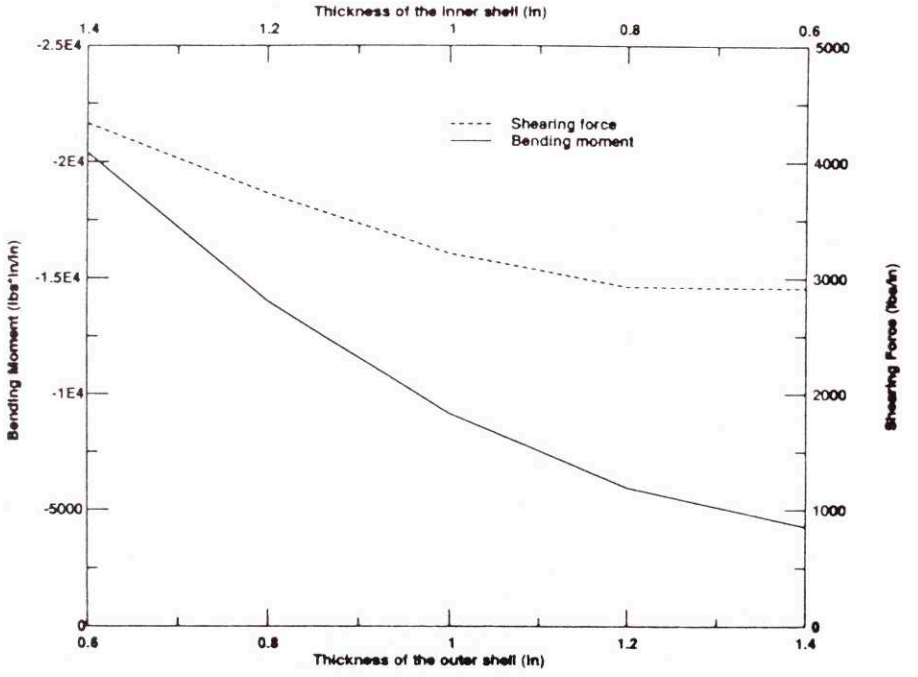

Fig. 46: Inner shell - Bending moments and shearing forces developed at the clamped ends

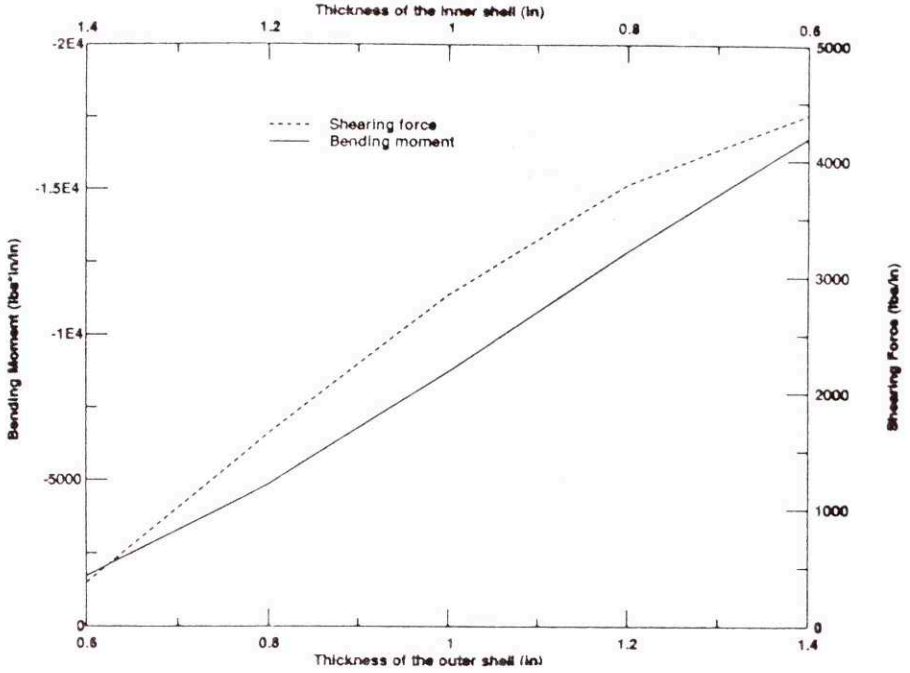

Fig. 47: Outer shell - Bending moments and shearing forces developed at the clamped ends

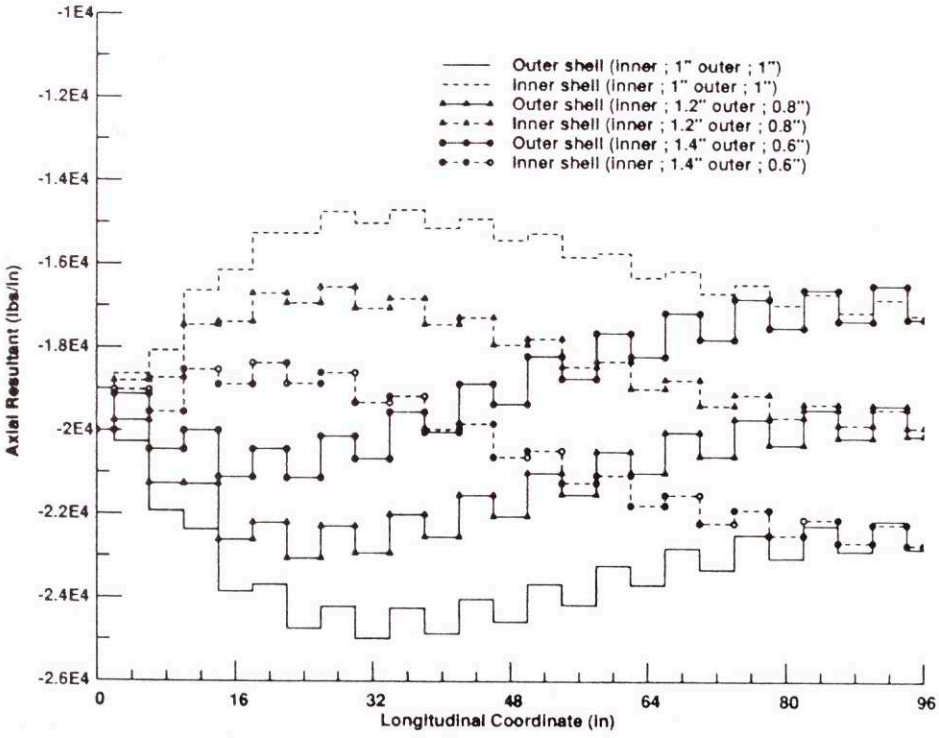

Fig. 48: Axial load distribution along the inner and outer shell

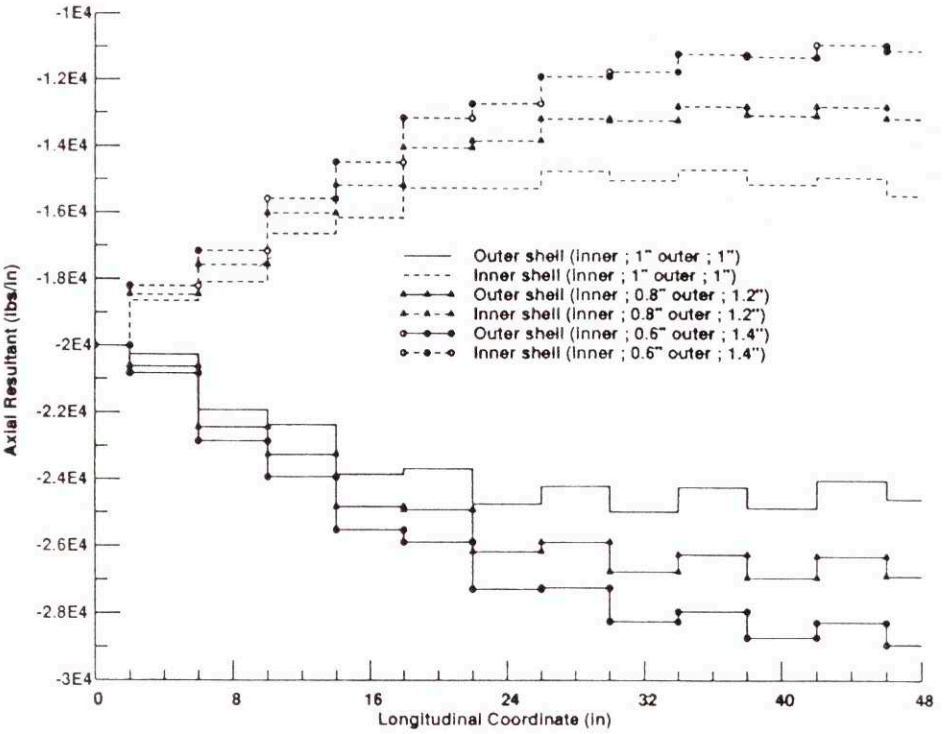

Fig. 49: Axial load distribution along the inner and outer shell

Appendix B

Evaluation of Energy Functions associated with Interactions between two Loads

We denote the coefficients $C_P = \frac{\pi R}{16\beta^3 D}$, $C_M = \frac{\pi R}{8\beta D}$, $C_{PM} = \frac{\pi R}{8\beta^2 D}$, $C_{pP} = \frac{\pi Rp}{4\beta^4 D}$, and $C_{pM} = \frac{\pi Rp}{4\beta^3 D}$.

We also denote functions $X_1 = \beta(x_i + x_j)$, $X_2 = \beta(x_i - x_j)$, $S_1 = \sin(X_1)$, $S_2 = \sin(X_2)$, $C_1 = \cos(X_1)$, $C_2 = \cos(X_2)$, $E_1 = e^{-X_1}$ and $E_2 = e^{X_1+X_2}$.

$$
\begin{aligned}
(I_s)_{P_{ij}} = \quad & C_P E_1 P_i P_j[-3S_1 + ((2X_2 - 3)E_2 - 2X_2)S_2 + (3 + 2X_1)C_1 \\
& +(3(E_2 - 2) - 2X_1)C_2] \\
(I_b)_{P_{ij}} = \quad & C_P E_1 P_i P_j[-S_1 - ((2X_2 + 1)E_2 - 2X_2)S_2 - 2X_1 C_1 \\
& +(E_2 + 2X_1 - 2)C_2] \\
(I_s)_{M_{ij}} = \quad & C_M E_1 M_i M_j[(2X_1 + 1)S_1 + (E_2 - 2X_2)S_2 + C_1 \\
& +((1 - 2X_2)E_2 - 2(1 + X_1))C_2] \\
(I_b)_{M_{ij}} = \quad & C_M E_1 M_i M_j[(3 - 2X_1)S_1 + (3E_2 + 2X_2)S_2 + 3C_1 \\
& +((2X_2 + 3)E_2 + 2(X_1 - 3))C_2] \\
(I_s)_{P_i M_j} = \quad & C_{PM} E_1 P_i M_j[X_1 S_1 + ((X_2 - 2)E_2 + X_1 + 2)S_2 + (X_1 + 2)C_1
\end{aligned}
$$

$$+(X_2E_2 - X_1 - X_2 - 2)C_2]$$

$$(I_s)_{P_jM_i} = C_{PM}E_1P_jM_i[X_1S_1 - ((X_2 - 2)E_2 + X_1 + 2)S_2 + (X_1 + 2)C_1$$
$$-(X_2E_2 + X_1 - X_2 + 2)C_2]$$

$$(I_b)_{P_iM_j} = C_{PM}E_1P_iM_j[-X_1S_1 - ((X_2 + 2)E_2 + X_1 - X_2 + 2)S_2 - (X_1 - 2)C_1$$
$$-(X_2E_2 - X_1 - X_2 + 2)C_2]$$

$$(I_b)_{P_jM_i} = C_{PM}E_1P_jM_i[-X_1S_1 + ((X_2 + 2)E_2 + X_1 + X_2 - 2)S_2 - (X_1 - 2)C_1$$
$$+(X_2E_2 + X_1 - X_2 - 2)C_2]$$

$$(I_s)_{pP_i} = -C_{pP}e^{-\beta x_i}P_i[(\beta x_i + 2)\sin(\beta x_i) + 2\cos(\beta x_i) - 2e^{\beta x_i}]$$

$$(I_b)_{pP_i} = C_{pP}e^{-\beta x_i}P_i\beta x_i\sin(\beta x_i)$$

$$(I_s)_{pM_i} = -C_{pM}e^{-\beta x_i}M_i[(\beta x_i + 3)\sin(\beta x_i) - \beta x_i\cos(\beta x_i)]$$

$$(I_b)_{pM_i} = C_{pM}e^{-\beta x_i}M_i[(\beta x_i - 1)\sin(\beta x_i) - \beta x_i\cos(\beta x_i)]$$

Bibliography

[1] Palaninathan, R. and P. Montague, *Studies of Dome-ended, Composite Construction, Cylindrical Vessels Subjected to Exdternal Pressure*, Proc. ICE Part II, pp 83 – 105, 1981.

[2] Montague, P., *Composite, Double-Skin Sandwich Pressure Vessels, in Shell Structures, Stability and Strength*, edited by R. Narayanan, pp 97 – 137, Applied Science Publishers LTD, New York, 1985.

[3] Flugge, W., *Stresses in Shells*, Springer-Verlag, Berlin, 1960.

[4] Bushnell, D., *BOSOR4: Program for Stress, Buckling and Vibration of Complex Shells of Revolution*, Structural Mechanics Software Series, Vol I, edited by N. Perrone and W. Pilkey, University Press of Virginia, Virginia, 1974.

[5] Irving H. Shames and Clive L. Dym, *Energy and Finite element Methods in Structural Mechanics*, McGraw-Hill, New York, 1985.

[6] A. C. Ugural, *Stresses in Plates and Shells*, McGraw-Hill, New York, 1981.

[7] A.E.H. Love, *A Treatise on the Mathematical Theory of Elasticity*, Dover Publications, New York, 1944.

[8] Timoshenko, S. and S. Woinowsky-Krieger, *Theory of Plates and Shells*, McGraw-Hill, New York, 1959.

[9] Timoshenko, S. and D. H. Young, *Elements of Strength of Materials*, D. VAN NOSTRAND COMPANY, INC., New York, 1968.

[10] Timoshenko, S., *Strength of Materials, Part II*, D. VAN NOSTRAND COMPANY, INC., New York, 1956.

[11] NAG, *Numerical Algorithms Group Fortran Library Routine, Mark 13*, NAG Ltd., 1988.

[12] Pulos, J.G. and Salerno, V.L., *Axisymmetric Elastic Deformations and Stresses in a Ring-Stiffned, Perfectly Circular Cylindrical Shell Under External Hydrostatic Pressure*, DTMB Report No. 1497, 1961.

[13] C. Chryssostomidis and N. A. Papadakis, *Buckling Analysis of Sandwich Shell Structures Subjected to Hydrostatic Load*, MIT Des. Lab. Report No. 91-20, 1990.

[14] MACSYMA, *MAC's SYmbolic MAnipulation system 414*, Symbolics, Inc., 1988.